

INFORMATION TO USERS

This material was produced from a microfilm copy of the original document. While the most advanced technological means to photograph and reproduce this document have been used, the quality is heavily dependent upon the quality of the original submitted.

The following explanation of techniques is provided to help you understand markings or patterns which may appear on this reproduction.

1. The sign or "target" for pages apparently lacking from the document photographed is "Missing Page(s)". If it was possible to obtain the missing page(s) or section, they are spliced into the film along with adjacent pages. This may have necessitated cutting thru an image and duplicating adjacent pages to insure you complete continuity.
2. When an image on the film is obliterated with a large round black mark, it is an indication that the photographer suspected that the copy may have moved during exposure and thus cause a blurred image. You will find a good image of the page in the adjacent frame.
3. When a map, drawing or chart, etc., was part of the material being photographed the photographer followed a definite method in "sectioning" the material. It is customary to begin photoing at the upper left hand corner of a large sheet and to continue photoing from left to right in equal sections with a small overlap. If necessary, sectioning is continued again — beginning below the first row and continuing on until complete.
4. The majority of users indicate that the textual content is of greatest value, however, a somewhat higher quality reproduction could be made from "photographs" if essential to the understanding of the dissertation. Silver prints of "photographs" may be ordered at additional charge by writing the Order Department, giving the catalog number, title, author and specific pages you wish reproduced.
5. PLEASE NOTE: Some pages may have indistinct print. Filmed as received.

University Microfilms International

300 North Zeeb Road
Ann Arbor, Michigan 48106 USA
St. John's Road, Tyler's Green
High Wycombe, Bucks, England HP10 8HR

77-15,336

HARRIS, Daniel Howard, 1942-
ICE MANTLES, AND THE SIZE OF INTERSTELLAR
GRAINS.

The University of Arizona, Ph.D., 1976
Physics, astronomy and astrophysics.

Xerox University Microfilms, Ann Arbor, Michigan 48106

ICE MANTLES, AND THE SIZE
OF INTERSTELLAR GRAINS

by

Daniel Howard Harris

A Dissertation Submitted to the Faculty of the
DEPARTMENT OF ASTRONOMY
In Partial Fulfillment of the Requirements
For the Degree of
DOCTOR OF PHILOSOPHY
In the Graduate College
THE UNIVERSITY OF ARIZONA

1 9 7 6

THE UNIVERSITY OF ARIZONA

GRADUATE COLLEGE

I hereby recommend that this dissertation prepared under my
direction by Daniel Howard Harris
entitled ICE MANTLES, AND THE SIZE OF INTERSTELLAR
GRAINS
be accepted as fulfilling the dissertation requirement for the
degree of Doctor of Philosophy

Nirbhaj Woolf
Dissertation Director

11/30/76
Date

As members of the Final Examination Committee, we certify
that we have read this dissertation and agree that it may be
presented for final defense.

T. G. Swihart
George Riebs
Pat A. Ammersted
[Signature]

11-30-76
11-30-76
12-2-76
12/7/76

Final approval and acceptance of this dissertation is contingent
on the candidate's adequate performance and defense thereof at the
final oral examination.

STATEMENT BY AUTHOR

This dissertation has been submitted in partial fulfillment of requirements for an advanced degree at The University of Arizona and is deposited in the University Library to be made available to borrowers under rules of the Library.

Brief quotations from this dissertation are allowable without special permission, provided that accurate acknowledgment of source is made. Requests for permission for extended quotation from or reproduction of this manuscript in whole or in part may be granted by the head of the major department or the Dean of the Graduate College when in his judgment the proposed use of the material is in the interests of scholarship. In all other instances, however, permission must be obtained from the author.

SIGNED: Daniel H. Harris

This work is dedicated to all those astronomers who are not only capable but are also humane, tolerant and supportive of their fellows.

ACKNOWLEDGMENTS

First, I would like to thank my parents for considerable patience and encouragement along the way, Lyle Supp, Dr. Godfrey Sill, Dr. Kenrick Day and Dr. William K. Hartmann for aid with the computations and access to unpublished results, Sarah Oordt and Gilbert McLaughlin who helped produce the manuscript and Michael Shainline for proofing the manuscript.

I would like to thank the Steward Observatory -- Lunar and Planetary Laboratory telescope scheduling committee for granting generous time on the 154cm Catalina telescope and for time on the Steward Observatory 2.3 meter telescope, the Kitt Peak National Observatory for providing computer time and the Steward Observatory and Lunar and Planetary Laboratory staff who aided in construction of the infrared detector system.

I would like to express deep gratitude to Dr. Per Aannestad, Dr. Donald R. Huffman and Dr. Stephen E. Strom for their useful discussions and encouragement and to Dr. Harold L. Johnson and Dr. Thomas L. Swihart for graciously consenting to serve on my examining committee. I would

particularly like to thank Dr. George Rieke and Dr. Neville Woolf for their useful discussions and for their aid in making the photometric observations. Without their continued patience and support this work would not have been completed.

TABLE OF CONTENTS

	Page
LIST OF TABLES	viii
LIST OF ILLUSTRATIONS	ix
ABSTRACT	xi
 CHAPTER	
I. INTRODUCTION	1
The Importance of Interstellar Grains . .	1
Our Ignorance of the Grain Properties . .	2
The Information Theory of Grain Properties	3
A Selection of Problems	5
Selecting Approaches to the Problems . . .	7
 II. THE RATIO OF TOTAL TO SELECTIVE ABSORPTION FROM THE CLUSTER DIAMETER METHOD	 10
Introduction	10
The Diameter Measures and Photometry . . .	10
The Computed Distance-Angular Diameter Relations	11
The Dependence on Angular Diameter on Cluster Type	18
The Revised Relations of Computed Distance to Angular Diameter	21
A Search for Other Correlations with Angular Diameter	25
Results Using the Revised Computed Distance-Angular Diameter Relations .	29
A Limit on the Galactic Longitude Variation of R	30
The Mean Reddening with Distance . . .	31
The Mean Value of R and Shrinkage with Reddening	31
A Measure of Large Particle Extinction	35

TABLE OF CONTENTS--continued

	Page
III. DESIGN OF THE INSTRUMENT FOR IR OBSERVATIONS	39
IV. INFRARED OBSERVATIONS OF A HEAVILY OBSCURED REGION SHOWING PECULIAR EXTINCTION	43
Introduction	43
Observations	44
The Extinction Curves	54
Extinction Curve Interpretations	67
The Ice Band Extinction Measures	71
V. ANALYSIS OF THE INFRARED OBSERVATIONS	83
The Density Dependence of Ice Extinction	83
The Estimated Ice Fraction	87
The Absolute Ice Extinction Efficiency	87
A Look at Grain Core Models	89
A Look at Grain Growth Processes	91
A Model of the Grain Composition	93
The Problem of Large Grains	96
The Grain Size Distribution Model	97
The Ice Mass Fraction	99
The Ice Mantle Thickness	102
The Mantle Contribution to Continuum Extinction	103
Why is There No Ice?	103
VI. SUMMARY	109
REFERENCES	112

LIST OF TABLES

Table	Page
I. Preliminary Mean Type Residuals in the Logarithm of the Angular Diameter	20
II. Final Mean Type Residuals and Linear Diameters	36
III. Filter Characteristics	41
IV. Magnitudes of Standard and Comparison Stars	46
V. Magnitudes of Program Stars	48
VI. Color Excesses of Stars With Optical Photometry	52
VII. Color Excess Ratios of Stars with Optical Photometry	56
VIII. Magnitudes of Ophiuchus Stars Having Far IR Photometry	59
IX. De-Reddened Magnitudes and Estimated Spectral Types of Ophiuchus Stars	62
X. Extinction and Color Excess Ratios	64
XI. Astronomical 3.1 μ m Band Data	72
XII. The Ice Band Extinction Measures	79
XIII. Grain Characteristics	98

LIST OF ILLUSTRATIONS

Figure	Page
1. The apparent angular diameter - photometric distance relations for Trumpler diameters and $R = 2.6$	12
2. The apparent diameter-distance relations for Trumpler diameters and for $R = 3.2$	13
3. The apparent diameter-distance relations for Trumpler diameters and $R = 3.8$	14
4. The apparent diameter-distance relations for Trumpler diameters and $R = 5.0$	15
5. The apparent angular diameter-photometric distance relations for Wallenqueist diameters and $R = 3.2$	17
6. The type corrected angular diameter-photometric distance relations for $R = 2.8$. .	22
7. The corrected angular diameter-distance relations for $R = 3.2$	23
8. The corrected angular diameter-distance relations for $R = 3.6$	24
9. Residuals of the corrected angular diameter ($R = 3.2$) plotted against galactic longitude .	26
10. E_{BV} as function of cluster distance ($R = 3.2$).	32
11. Distance dependent cluster shrinkage with reddening for various R values	33
12. The extinction curves for stars with optical region photometry and van de Hulst 15	55
13. The mean Ophiuchus extinction curves in the infrared	65

LIST OF ILLUSTRATIONS--continued

Figure	Page
14. The estimated ice band extinction profile . . .	76
15. The dependence of the relative ice extinction on E_{HK}	81

ABSTRACT

An examination of previously reported large R ($\equiv A_V/E_{BV}$) variations using the cluster diameter method shows that the local galactic mean value of R is $R = 3.15 \pm 0.20$, and that on a scale comparable to the width of the local spiral arm there is no substantial systematic variation in R .

Infrared photometry of eleven strongly obscured stars shows that near ρ Oph the extinction is distinctive with a large R value and inferred large grain size. Furthermore, for $A_V \lesssim 25$ mag there is little or no ice band ($3.07\mu\text{m}$) extinction, yet for the more heavily obscured stars the ice extinction to E_{HK} ratio is ~ 0.30 . There seems to be a dichotomy in ice band strength at an onset local dust density of ~ 5 mag/pc in E_{HK} . A model assuming silicate core grains and cosmic abundances shows that below the onset density the observed ice extinction is ~ 350 times less than the expected maximum and that above the onset density it is ~ 30 times less than the expected maximum. Since condensation of ice is believed to occur at $\sim 17^\circ\text{K}$, the observed $\sim 50^\circ\text{K}$ dust temperature may explain the generally low ice abundance.

CHAPTER I

INTRODUCTION

The Importance of Interstellar Grains

Knowledge of the interstellar grains is important to a wide range of ongoing research in various areas of astronomy. The interstellar grains dominate the opacity of interstellar space over a large wavelength range, influencing the distance and flux measures of both galactic and extragalactic sources (see reviews by Wickramasinghe and Nandy 1972; Aannestad and Purcell 1973). Grain-caused opacity may also perturb the development of protostellar and preplanetary systems (Reeves 1972; McNalley 1973; and Cameron 1975). Grains may thereby influence the critical balance which determines the rate of star formation, the stellar mass spectrum, the binary frequency, and the abundance and chemistry of planetary bodies. The grains also cause interstellar polarization (Serkowski 1973; Serkowski, Mathewson, and Ford 1975) which can be used as a tracer of the galactic magnetic field (Mathewson 1968, Serkowski 1973), a vital element in the study of cosmic rays and the more general problem of galactic structure, dynamics and evolution. An area of intense current

interest is the study of interstellar molecules and gas chemistry (Gordon and Snyder 1973, Herbst and Klemperer 1976), where the reactions of gas atoms on grain surfaces and the growth or destruction of grains may be important both to the chemical composition and to the energy exchange equilibria of the gas and dust.

Our Ignorance of the Grain Properties

Despite the importance of knowledge of the interstellar grains, our present state of knowledge may be described as rudimentary. We have only crude knowledge of the grain composition and even less exact information about the grain size distribution (Greenberg 1968; Wickramasinghe and Nandy 1972; Aannestad and Purcell 1973). Clearly there is no set of model grain properties which has a validity independent of model structure. Each of the several grain composition models has a means of producing grains and is capable of explaining most observations, but each also has difficulty in explaining some of the pertinent observations.

One major difficulty in making an accurate grain model is that the wavelength dependent complex refractive index of candidate materials under interstellar conditions is often poorly known (Irvine and Pollack 1968; Huffman and Stapp 1973; Greenberg 1973). A more fundamental difficulty is that the theoretical physics (usually the Mie

theory for spherical particles) which is used in computing the attenuation and scattering of light, is only an approximation to the real grains. Real grains may be quite different in their crude shape, many have surface roughness, and may even be variable in composition from grain to grain, and within each grain. An understanding of the limitations of the theory as applied to real particles (Sinclair 1947; Bardwell and Sivertz 1947; LaMer 1948; Heller, Epel and Tabibian 1954; Grumprecht and Sliepcevich 1953; Huffman and Stapp 1973; Day and Huffman 1973; and Huffman 1975) demonstrates the restricted utility of the current grain models. Another fundamental difficulty is that, while knowledge of the complexity of the real grain assemblage is essential if one is to construct a comprehensive and accurate model, the observations give no direct indication of the grain assemblage complexity (Aannestad and Purcell 1973).

The Information Theory of Grain Properties

In an abstract and fundamental sense, solving for the grain properties may be thought of as analogous to solving n equations in m unknowns. If $n \geq m$ then a unique solution exists, but if $m > n$ then there is an infinity of pseudo solutions but no unique answer. Similarly, if the grain assemblage is so complex that a

complete description requires more independent information elements than are retrievable from the observations ($m > n$), then there is no unique solution for the complete set of grain properties. Instead, it may be possible to obtain a valid solution for a subset of the grain properties, a subset whose information content matches that which is retrievable from the observations. Such a solution would be the best possible. On the other hand, if the grain assemblage contains less information than can be retrieved from the observations, then the appropriate complexity in the model is that which matches the actual complexity of the grains ($m = n$). A model less complex than appropriate may be accurate as far as it goes, but a model which is excessively complex, although it might be made to fit the observations, is necessarily a pseudo solution analogous to $m > n$.

From these arguments it should be clear that in order to have confidence in the accuracy of a grain assemblage model one must know that either the model has the appropriate complexity or that it has less than the appropriate complexity. Since the observations do not yield an unambiguous measure of the complexity of the real grain assemblage (Wickramasinghe and Nandy 1972; Aannestad and Purcell 1973), one can either go through the laborious

process of making many models with the hope of discovering some clear indication of the appropriate complexity, or one may choose to be sure that the model is less complex than appropriate by following a simple and direct approach, e.g., spectroscopy. I have chosen the sure and simple approach.

A Selection of Problems

Having chosen the simple approach, it is necessary to select questions for study which require only observation and straightforward analysis to obtain specific meaningful answers. At the outset of this project, among the many topics of interest to students of galactic structure and the interstellar dust was one which excited more interest than the rest: The question of the reality of the anomalously large values of R ($\equiv A_V/E_{BV}$) and the apparent galactic longitude variation of R found by Johnson (1968). [R is defined as the ratio of the total extinction for visual light ($\lambda = 0.55\mu\text{m}$), A_V ; to the color excess, the difference in extinction at the blue ($\lambda = 0.44\mu\text{m}$) and visual wavelengths, $E_{BV} = A_B - A_V$.] The recent discovery of large R values in dark cloud regions (Carrasco, Strom and Strom 1973) may relate to Johnson's locally large R values and the regional variation of

λ_{\max} of polarization noted by Serkowski et al. (1975) may relate to Johnson's inference of a longitude dependence of R. Thus the question of the large R values is recognized as one of importance and one which seems suited for straightforward analysis.

Another question of long standing interest is the question of the grain composition. Are the often invoked theoretical arguments for ice grains (Greenberg 1968) supported by spectral observations, or do arguments favoring graphite or silicate materials prevail (Wickramasinghe 1967, Huffman 1975)? This question is ideally suited for direct observational test. Furthermore, the variation of R and the grain composition are two related questions. Both relate to basic assumptions about the properties of the interstellar grains. The question of large R values relates to the conventional assumption that there are no large grains causing grey extinction and the grain composition is a property which is commonly assumed. The two questions are also related in that the large R values presumably imply the presence of larger than normal grains and perhaps the action of grain growth, and the prime candidate for the growth material is usually taken to be ice (Greenberg 1968).

Selecting Approaches
to the Problems

In establishing the apparent regional variations of R , Johnson (1968) used measures by the variable extinction method, the color difference method and the cluster diameter method. His variable extinction results were questioned by Becker (1966), who raised serious doubts about the utility of the variable extinction approach and Johnson's use of it. When I plotted Johnson's estimates of R against distance for each association, I found a significant decline in R with distance which is reminiscent of the effect described by Walker (1962), wherein artificially large R values are found for nearby clusters due to the inclusion of stars of differing distances. Becker (1966) elaborated on this effect and included analyses of sample associations. Furthermore, Isobe (1968), MacConnell (1968) and Simonson (1968), and later Garrison (1970) and Crawford and Barnes (1970) did variable extinction studies resulting in normal R values at odds with the results of Johnson (1968). The apparent difficulties with the use of this method argued persuasively against my use of it.

Johnson's color difference results have also been questioned, first by Johnson (1967), then by Grubisich.

(1968), Lee (1970), and by Schultz and Weimer (1975). The difficulty in knowing exactly how to extrapolate from the longest observed wavelength to infinite wavelength, plus the difficulty in obtaining high quality photometry of a sufficiently large sample of stars to make a useful contribution, and the large quantity of already available photometry, persuaded me not to try a general application of this approach. However, since it was recognized that a limited application of the color difference method to certain unusual regions might be very useful in clarifying the question of small regions with large R values, it has been used here for that purpose.

The existence of a large and uniform sample of cluster diameter measures and corresponding photometry (see Chapter II), plus the fact that the cluster diameter method overcomes the uncertainty in extrapolating to infinite wavelength and permits the measurement of large particle extinction, persuaded me of the importance and utility of this approach.

The obvious approach to the question of the ice abundance is spectroscopy. However, as we shall see in Chapter III and Chapter IV, filter photometry proved quite effective for measuring the ice abundance. Also,

the use of a photometric system permitted selected application of the color difference approach.

In summary then, I chose to approach the problem of the large R values (and the related question of particle size variations) in the general interstellar medium by the cluster diameter method and in the dense dark regions by the photometric method, and I chose to approach the question of the grain composition by means of narrow band photometric measurements.

CHAPTER II

THE RATIO OF TOTAL TO SELECTIVE ABSORPTION FROM THE CLUSTER DIAMETER METHOD

Introduction

Of the methods available for measuring the interstellar extinction, only the cluster diameter method can measure the grey extinction of large particles (Johnson 1968). This method is therefore potentially very useful. To fully realize this potential one must collect accurate diameter measures and photometry for a large, homogeneous sample of open clusters.

The Diameter Measures and Photometry

Trumpler (1930) and Wallenquist (1959) have published the only large and uniform sets of open cluster diameter measures. I have made an effort to assemble the necessary photometry of these clusters. Photometric data tabulated by Johnson et al. (1961), Becker (1963), and Hagen (1970) have been examined and inter-compared. Where possible the cluster color-magnitude diagrams were studied. Only 156 of the clusters had well determined distance moduli and color excesses. These were transformed to the

UBV system. The photometric data were then used to compute the cluster distances for various assumed values of $R(\equiv A_V/E_{BV})$. For the purposes of this paper I consider clusters with $E_{BV} < 0.15$ to be unreddened. Such small color excesses with normal values of R change the distance modulus by less than a half magnitude.

I have omitted a listing of the clusters and a detailed discussion of the transformations, and will later omit other tabulations of the data because including them here would complicate the discussion and take the focus away from the important question of the mean cluster diameters and the implied mean value of R . (A tabulation of the data and a more detailed discussion of the analysis will be published elsewhere.)

The Computed Distance-Angular Diameter Relations

Figures 1, 2, 3, and 4 present the log distance-log apparent angular diameter data for Trumpler's diameters. The (X) points are clusters with $E_{BV} < 0.15$ and the (+) points are clusters with $E_{BV} \geq 0.15$. The curves are least squares quadratic fits to the points assuming all error is in the angular diameters. The dashed curves fit the (X) points, the solid-dashed curves fit the (+) points and the solid curve fits all the points. It is

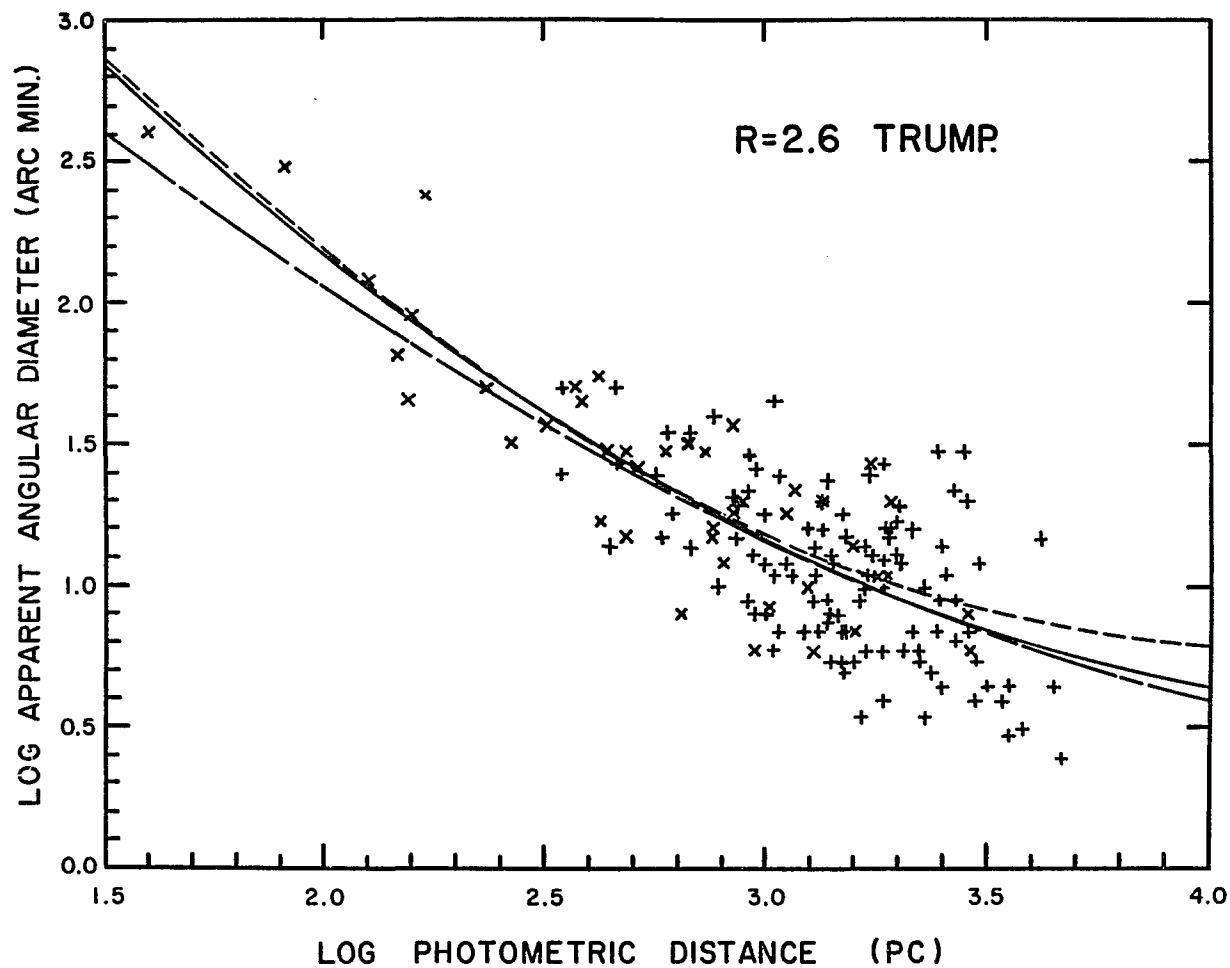


Figure 1. The apparent angular diameter-photometric distance relations for Trumpler diameters and $R = 2.6$.

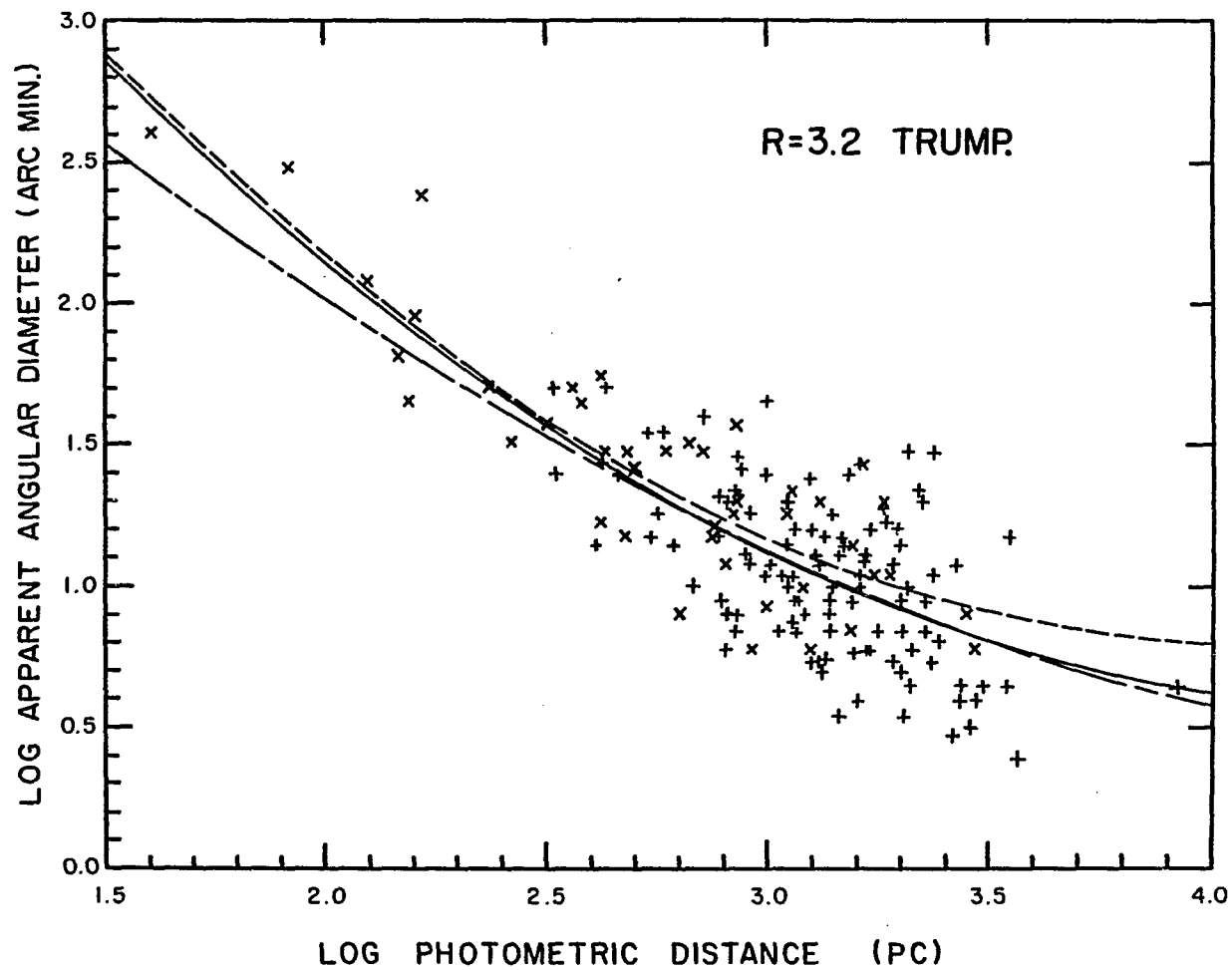


Figure 2. The apparent diameter-distance relations for Trumpler diameters and for $R = 3.2$.

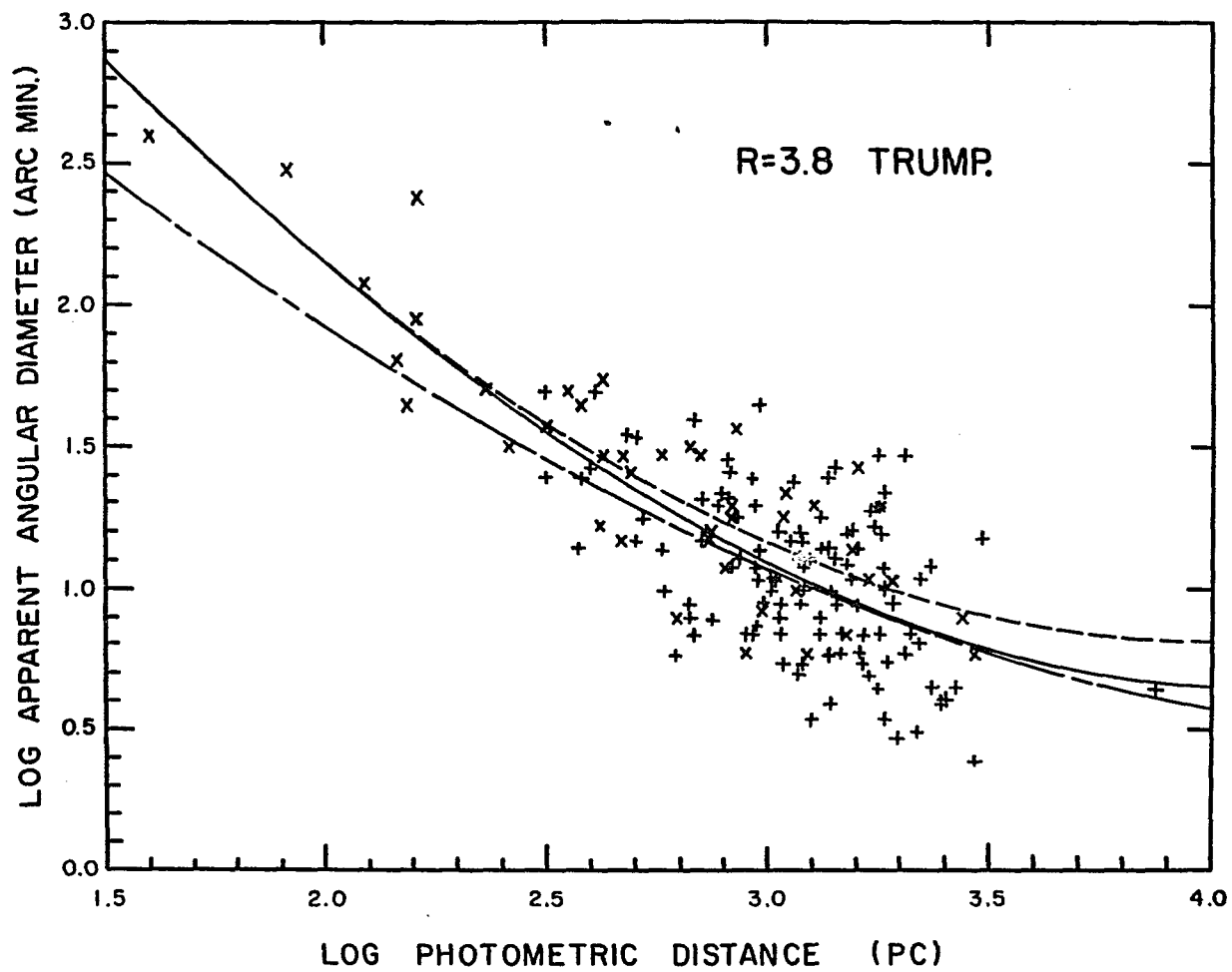


Figure 3. The apparent diameter-distance relations for Trumpler diameters and $R = 3.8$.

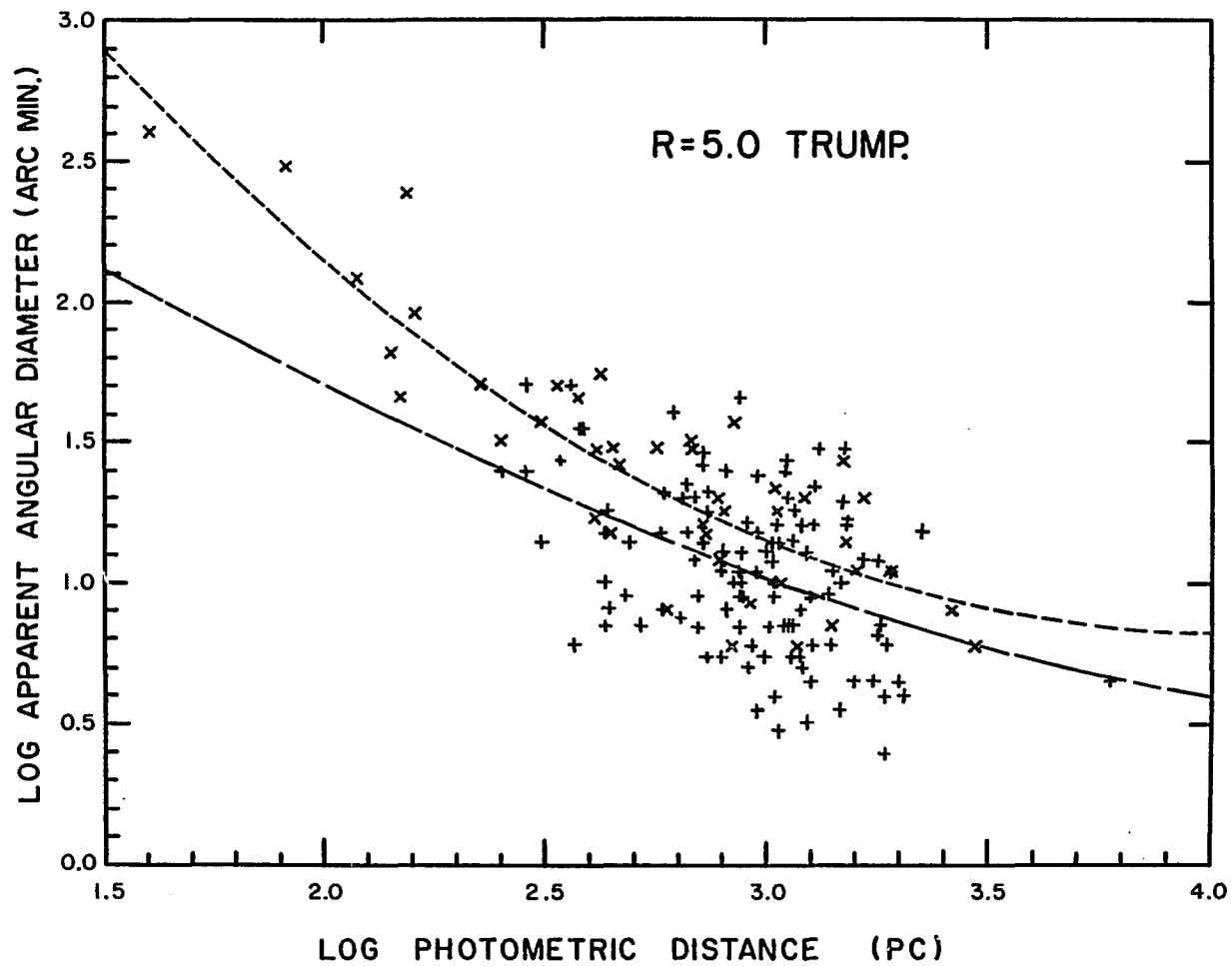


Figure 4. The apparent diameter-distance relations for Trumpler diameters and $R = 5.0$.

evident that the reddened and unreddened clusters follow nearly the same computed distance-apparent diameter relation. This is confirmed by the near agreement of the least squares quadratic fits. Note that because of the large scatter in apparent diameter the general distribution of points does not change rapidly with R . The best agreement of the positions of the reddened and unreddened clusters on the diagrams seems to be when $R = 3.2 \pm 0.4$.

The distance-apparent diameter plots for Wallenquist's diameters look nearly the same as the Trumpler plots except that there are fewer points. Figure 5 presents the distance-apparent diameter data for Wallenquist's diameters and $R = 3.2$.

There are two obvious peculiarities in the computed distance-apparent diameter relations. First, the mean slope of the fits is larger than negative one and there is a noticeable curvature in the fits suggesting that effects are present other than simply the reduction of apparent size with distance. Second, the mean cluster size seems to decrease with increasing E_{BV} . This is shown by the apparent difference between fits to reddened and unreddened clusters. (The apparent reddening dependent differences in the fits are not significant outside the range $3.5 > \log r > 2.4$, where r is in parsecs.) However,

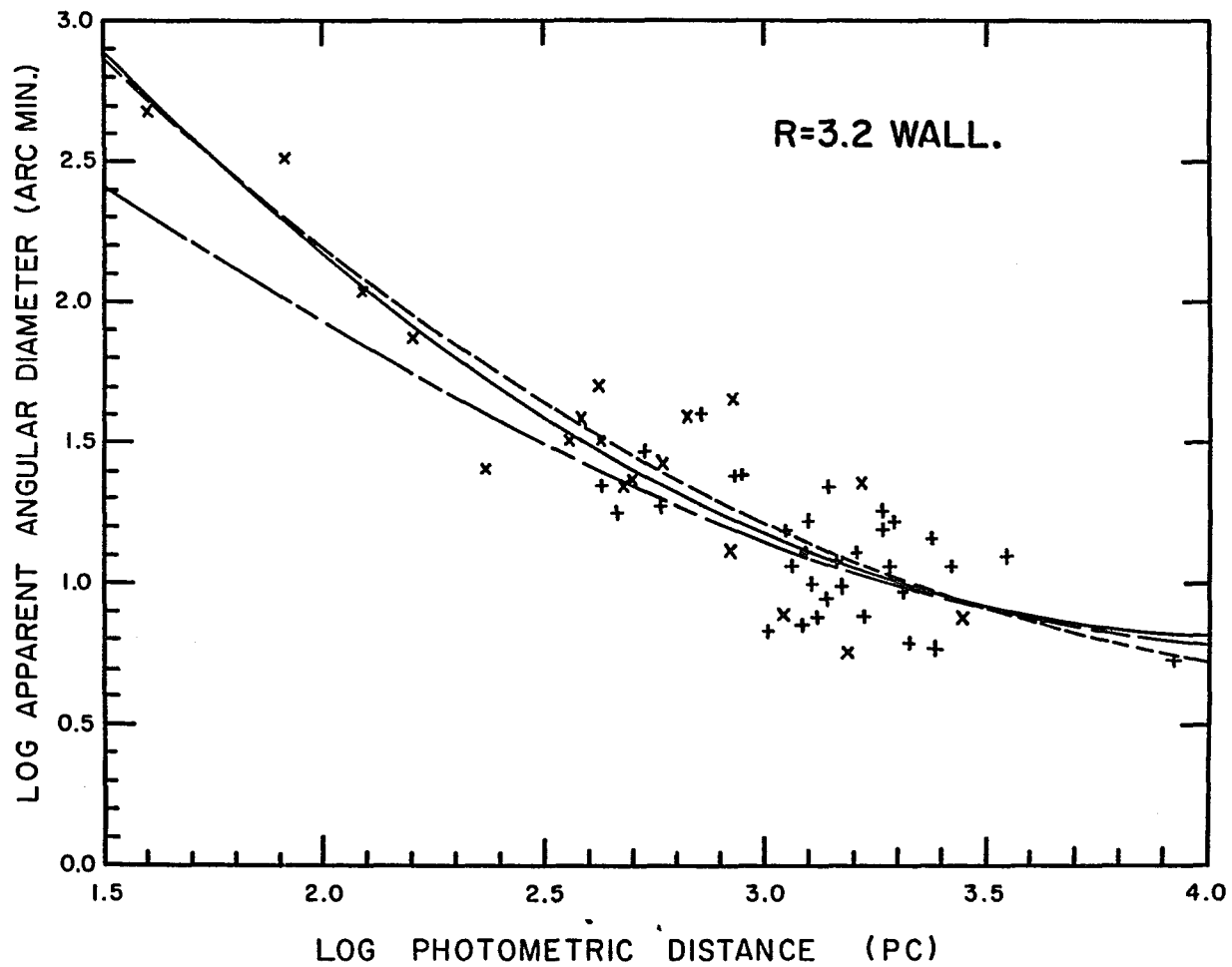


Figure 5. The apparent angular diameter-photometric distance relations for Wallenqueist diameters and $R = 3.2$.

for $R \lesssim 3.0$ the statistical uncertainties in the fits are comparable to the separation of the fits, showing that there is no significant dependence of mean cluster size on E_{BV} if $R \lesssim 3.0$. Consider for example Figure 1, where it is assumed $R = 2.6$, there it is apparent that there is no significant difference between the fits to the reddened and unreddened clusters. Unfortunately, the measurement of apparent shrinkage with increasing E_{BV} cannot be separated from the problem of finding the best value of R (later papers will discuss this in detail). Because of the difficulty in studying these effects, particularly when large residuals are present, it seems best to first attempt to reduce the size of the diameter residuals. In order to do this I conducted a search for dependences of the apparent diameters on other variables.

The Dependence of Angular Diameter on Cluster Type

A dependence of apparent diameter on cluster type is not unexpected (Trumpler 1930, Lynds 1967). Trumpler (1930) classified clusters according to concentration, ranging from type I which is strongly concentrated and well detached from the star field to type IV which is not well detached; and according to richness or number of recognizable members, ranging from p (poor) with less

than 50 members to *r* (rich) with more than 100 apparent members. To test for a type dependence I have computed mean residuals in the logarithm of the apparent angular diameter for each type relative to the least squares fits to all the clusters. These residuals show that Trumpler's diameters depend significantly on both concentration class and richness class. (Wallenquist's diameters in contrast show no significant dependence on concentration.) Residuals for all clusters of a particular concentration class and richness class have been averaged, except for those clusters that markedly deviate from the mean or their type, and show some other notable peculiarity such as association with emission nebulosity. (This may eliminate from the mean, those clusters with truly outstanding *R* values.)

Table I presents the preliminary mean type residuals for Trumpler types and for assumed *R* values of 2.8, 3.2, and 3.6. In general, cluster diameter increases with the number of members from *p* to *m* to *r* and decreases with concentration from IV to I. Similar trends in cluster size were noted by Trumpler (1930) and by Lynds (1967).

Because certain cluster types differ in mean E_{BV} from the mean E_{BV} of all the clusters, their mean type

TABLE I

Preliminary Mean Type Residuals
in the Logarithm of the Angular Diameter

$R = 2.8$

	I	II	III	IV
r	+0.12	+0.12	+0.27	+0.46
m	-0.08	-0.03	+0.25	+0.32
p	-0.17	-0.18	-0.01	+0.16

$R = 3.2$

	I	II	III	IV
r	+0.13	+0.13	+0.28	+0.45
m	-0.08	-0.03	+0.25	+0.31
p	-0.18	-0.18	-0.01	+0.16

$R = 3.6$

	I	II	III	IV
r	+0.13	+0.13	+0.28	+0.44
m	-0.07	-0.03	+0.26	+0.29
p	-0.18	-0.18	0.0	+0.16

residuals contain terms like $C \cdot \Delta E_{BV}$, where ΔE_{BV} is this color excess difference. Assuming in turn that each value of R is correct, then one can estimate the shrinkage coefficient C , by the separation of the least squares fits. The preliminary value (for $R = 3.2$) is $C = -0.073 \pm 0.04$. The largest value of $|\Delta E_{BV}|$ is 0.26 so at most the correction to $\log D'$ is ± 0.02 , which is only marginally significant. Therefore I have not corrected the mean type residuals for the $C \cdot \Delta E_{BV}$ effect.

The Revised Relations of
Computed Distance to
Angular Diameter

Figures 6, 7, and 8 present the distance-apparent diameter data corrected for dependence on Trumpler type. New least squares fits are also shown. The curvature in the new fits is slightly diminished while the apparent shrinkage with color excess is increased. Neither of these changes is very significant when the large size of the initial residuals is considered. The best agreement between the reddened and unreddened clusters still seems to be near $R = 3.2$.

With the type dependence removed, the Trumpler diameters have noticeably smaller residuals. (The mean diameter residuals decrease from $\sigma^2 = 0.057$ to $\sigma^2 = 0.031$.) In fact, the revised Trumpler diameters have

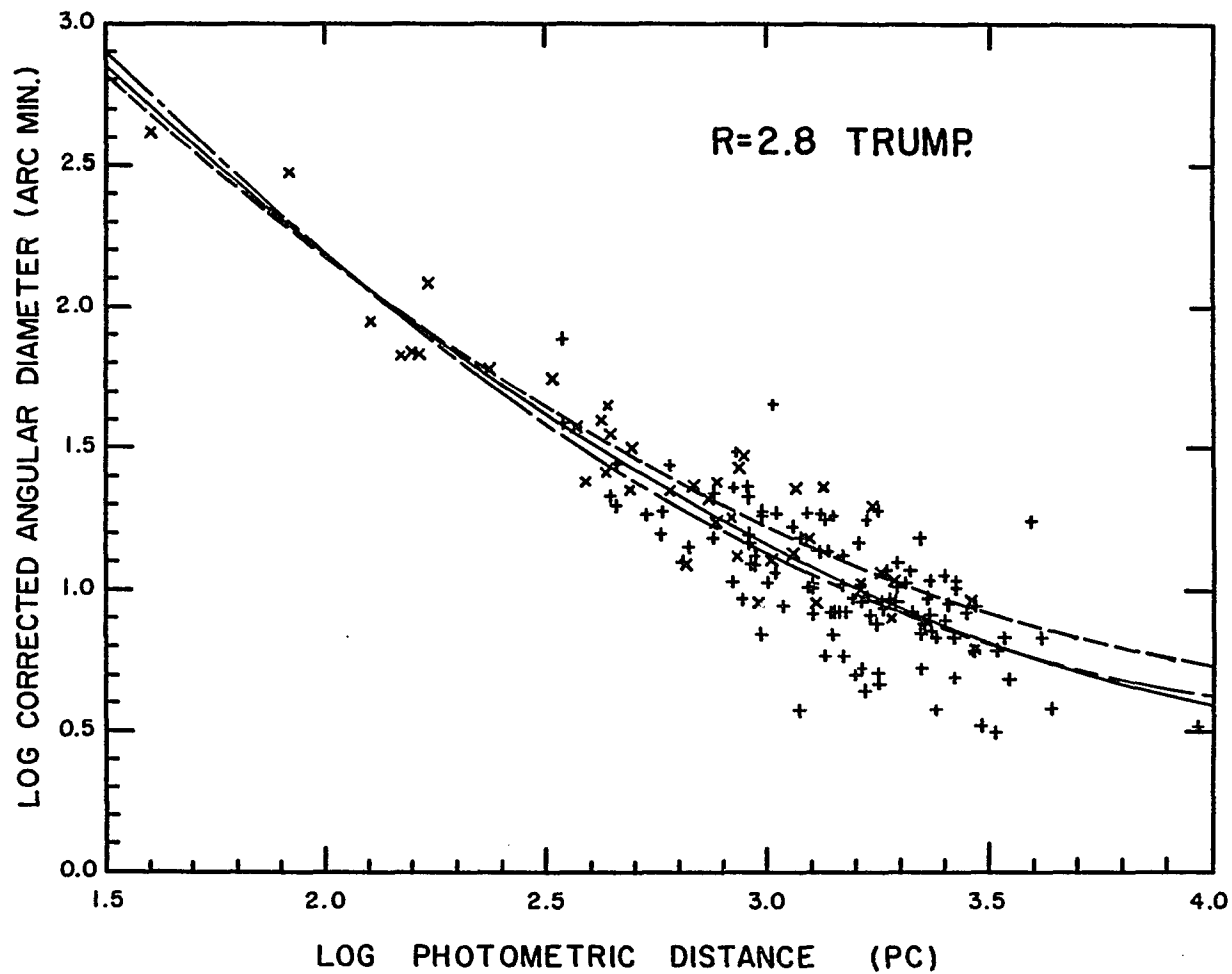


Figure 6. The type corrected angular diameter-photometric distance relations for $R = 2.8$.

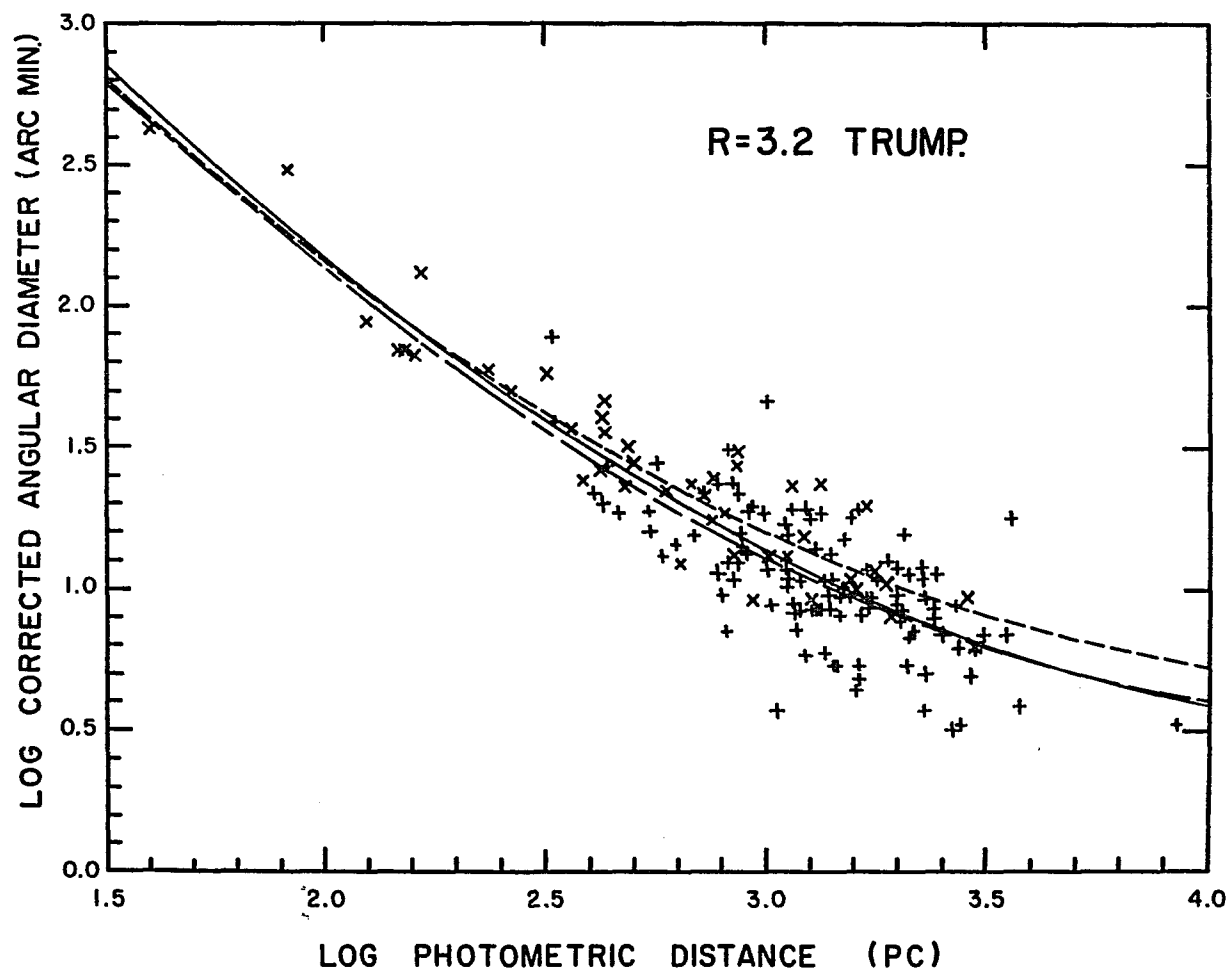


Figure 7. The corrected angular diameter-distance relations for $R = 3.2$.

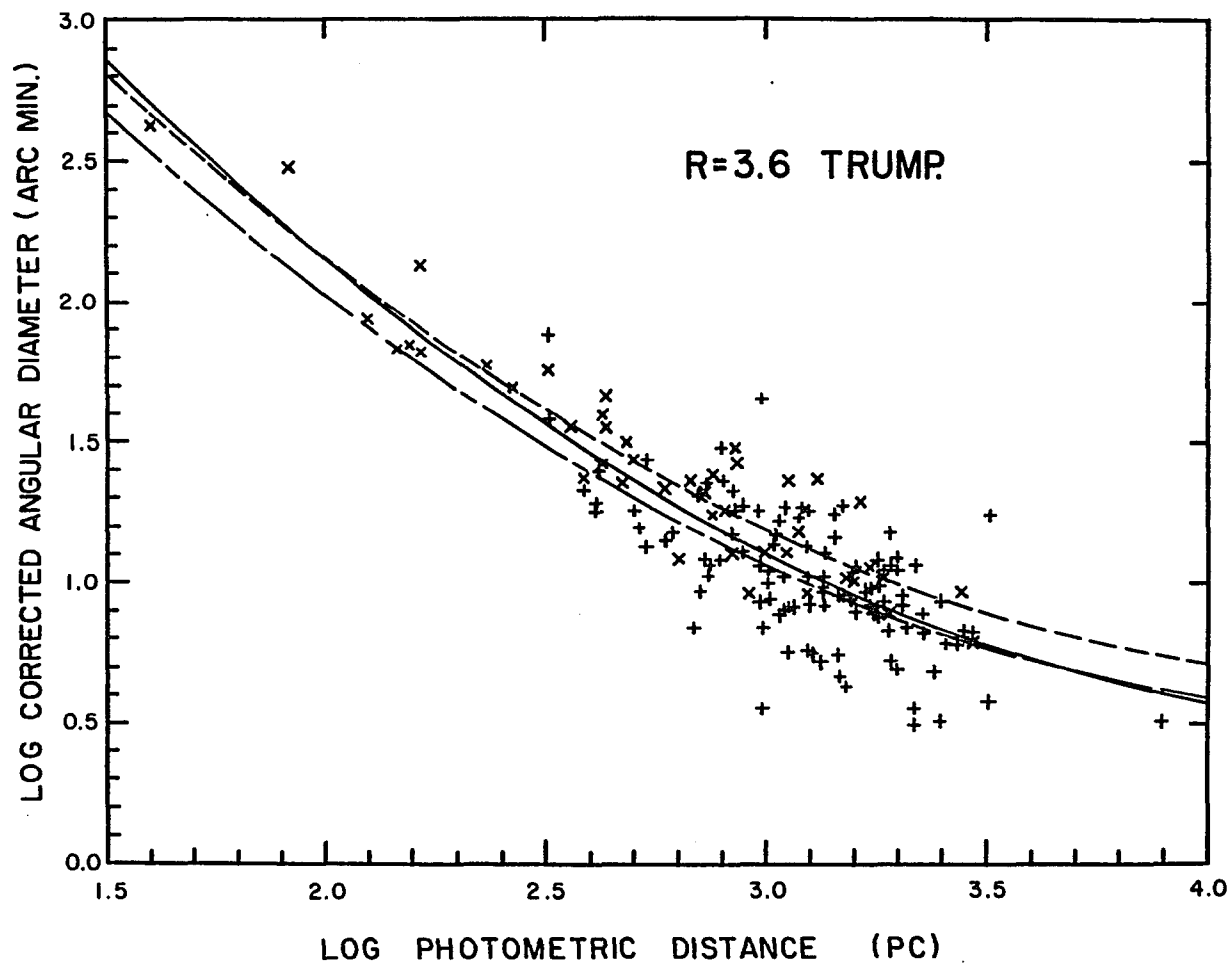


Figure 8. The corrected angular diameter-distance relations for $R = 3.6$.

smaller residuals than the Wallenquist diameters. The larger residuals of the Wallenquist diameters and their smaller number make them unsuited for further study here.

The remaining Trumpler diameter residuals are still large compared to the residuals which might come from errors in the distance moduli. Therefore we need to search further for diameter dependences.

A Search for Other Correlations with Angular Diameter

Figure 9 presents the residuals in the type corrected Trumpler diameters plotted against galactic longitude. As the residuals do not vary rapidly with R , I have assumed $R = 3.2$. The circled points represent clusters which were not included in the computation of the mean type residuals. It is clear that within the sensitivity limits of the present data there is no large systematic longitude variation of cluster diameter residuals. Further graphical analysis of the residuals of the revised Trumpler diameters shows no significant variation with distance from the galactic center, spiral arm number or spectrum of earliest member star. Combinations of these variables also yield no apparent relations.

It may seem that we have exhausted the variables which might relate to cluster diameter, but we have as

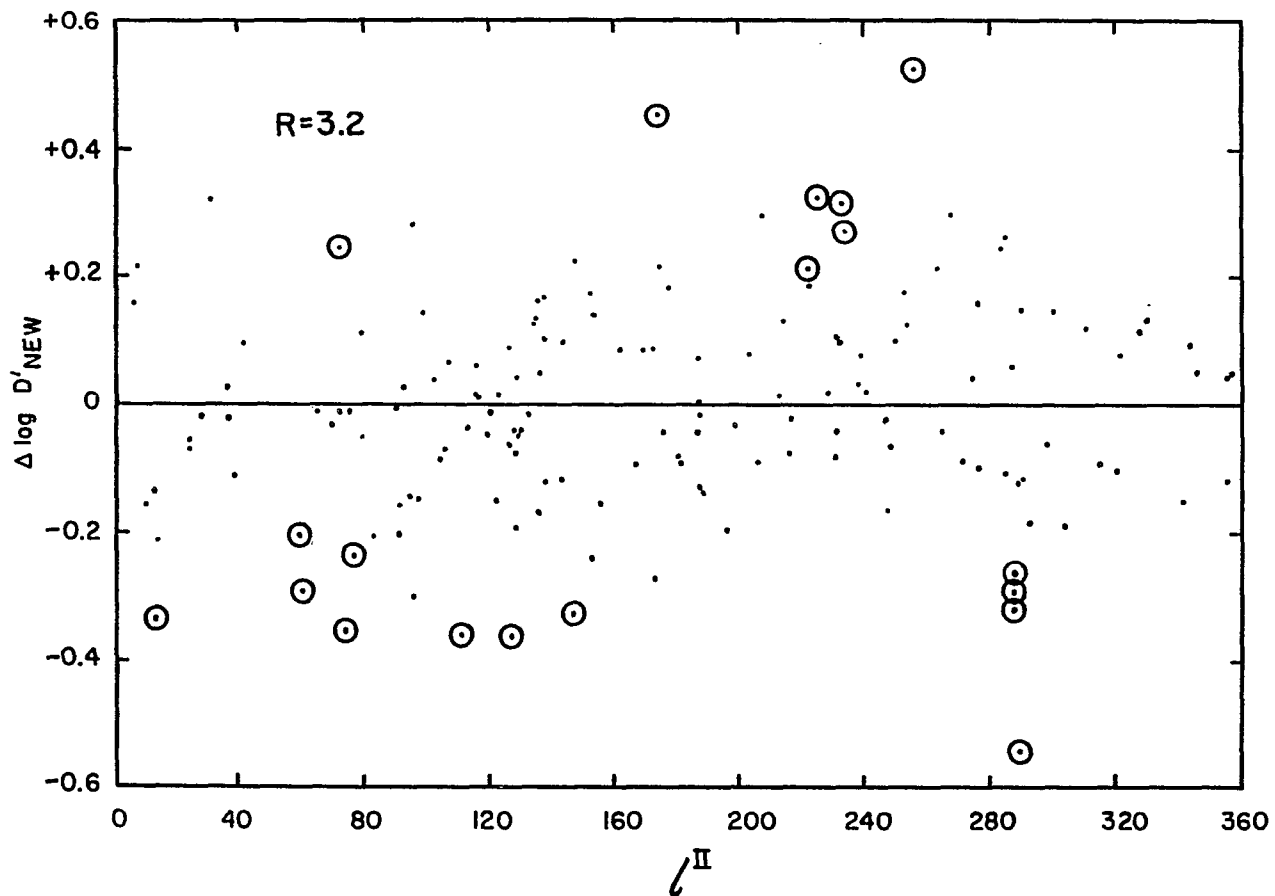


Figure 9. Residuals of the corrected angular diameter ($R = 3.2$) plotted against galactic longitude.

yet considered only variables which might relate to the true diameter of the cluster. As we shall see there seem to be other effects which change the apparent cluster size. For example, diameter measures made from material which does not have a sufficiently faint and uniform limiting magnitude or diameter measures made for stars of variable brightness ratio fainter than the brightest members will show increased residuals due to limiting magnitude effects. (Trumpler's measures probably show no such effects.)

An effect which is undoubtedly present, is that for clusters of increasing distance the cluster stars become fainter and less recognizable against the background of the more abundant faint field stars. This is a consequence of the fact that the fainter cluster members are generally spread over a larger area than the brighter ones (Trumpler 1922; Trumpler 1930). On the computed distance-apparent diameter plots the apparent decrease in inferred linear diameter with increasing distance and field star background yields a slope greater than minus one. However, for clusters at large enough distances the brighter field stars are ignored with the result that there is a distance beyond which the diameter is not further affected. Such an apparent cluster shrinkage with increasing distance and field

star numbers seems to be present (see Figures 6, 7 and 8) for clusters out to the distance $\log r \approx 2.8$.

Another noteworthy effect involves regional or distance dependent variations in the field star density. Near the cluster boundary the number density of stars falls off slowly. As a consequence, variations in the background of field stars may strongly influence the apparent cluster diameter. Trumpler (1922) has given a cluster density profile from an average of several clusters. The boundary slope is about one to five ($dN/dr = -0.20$) normalized to a radius of one and a central density of one. The average field star density is about one-quarter of the cluster's central density. With such a boundary slope and field star density, a fractional change in the field star density, produces a like fractional change in the apparent diameter. Such an effect seems appropriate to explain the increasing size of the inferred linear diameters of clusters beyond the average computed distance $\log r = 2.8$. To explain this variation there should be a locally high star density out to an average distance $r \approx 600\text{pc}$, beyond which the density declines significantly. General star counts averaged over galactic longitude given by McCuskey (1965) do indeed show a marked decline beyond $r \approx 600\text{pc}$, reaching about half of

the local density. Such a decline in star density is just about the right amount to explain the curvature of the quadratic fits and the apparent size increase of clusters beyond $r \approx 600\text{pc}$.

Unfortunately, these effects are not thoroughly understood, nor are there adequate supplementary data available (e.g., background star densities for each cluster), to aid in their removal. Therefore I found it necessary to assume that the mean computed distance-apparent diameter relations presented in Figures 6, 7, and 8 are the best practical representations of the mean variation of apparent diameter with true cluster distance (assuming in turn that each R value is correct).

Results Using the Revised Computed Distance-Angular Diameter Relations

The precision with which systematic or regional R variations can be delimited using residuals from the mean relations between computed distance and angular diameters is determined principally by the apparent variance of the cluster diameters. Unfortunately, as should be apparent from the above discussion, this variance is a composite of several effects, including true variance of cluster linear diameters, apparent diameter variance due to fluctuations in the field star background, and perhaps other unrecognized

effects. In principle these effects are inseparable. However, one can set an upper limit on the variations of R by assuming the diameter residuals are entirely due to variations in R .

The entire variance (mean residual from each mean relation) in the logarithm of the diameter is ~ 0.16 . Using this number, for clusters having a reddening typical of the mean ($E_{BV} \cong 0.33$), the variance of R is $\sigma_R \lesssim 2.4/\sqrt{n}$, where n is the number of clusters in the sample. For example, if $n = 156$ (all clusters in the current study) then $\sigma_R \lesssim 0.2$. For a quarter of the sample (as would be the case for a 90° longitude interval) $\sigma_R \lesssim 0.4$. It should be apparent from these numbers that substantial variations of R about the mean are not detectable in small samples of clusters and that to obtain a reasonably accurate estimate of the derivation $[(R - \bar{R})$, with $\sigma_R \lesssim 0.4]$ one needs to use a sample with $n \gtrsim 40$. Such a sample covers a region with a scale comparable to the width of the local spiral arm. Thus, systematic and regional variations in R can be determined only to ± 0.4 .

A Limit on the Galactic Longitude Variation of R

Applying this analysis to the question of the longitude variation of R , one finds that in 90° longitude

intervals the variation of R is ± 0.4 about the mean (still assuming all the variations in diameter are due to variations in R), a value comparable to the uncertainty of $(R - \bar{R})$ in each longitude interval. Thus the numbers confirm the previously noted absence of a significant longitude variation of R (see again Figure 9).

The Mean Reddening with Distance

Figure 10 presents the computed distance-color excess plot for all clusters and the assumption $R = 3.2$. The (X) points are clusters with both Wallenquist and Trumpler diameters. The (+) points have only Trumpler diameters. The sloping solid line is the estimated mean reddening-distance relation and the dashed lines show the estimated normal variations of the relation. A series of such plots for various assumed R values shows that E_{BV} increases more linearly with distance for R values near 3.2. If $R \simeq 3.2$ then $E_{BV}(r) = (0.28 \pm 0.05 \text{ mag/kpc})$.

The Mean Value of R and Shrinkage with Reddening

Figure 11 presents the distance dependence of the difference between the least squares fits to the reddened and unreddened clusters for various assumed R values. If each R value is in turn assumed to be correct, then the fit differences represent the reddening caused cluster

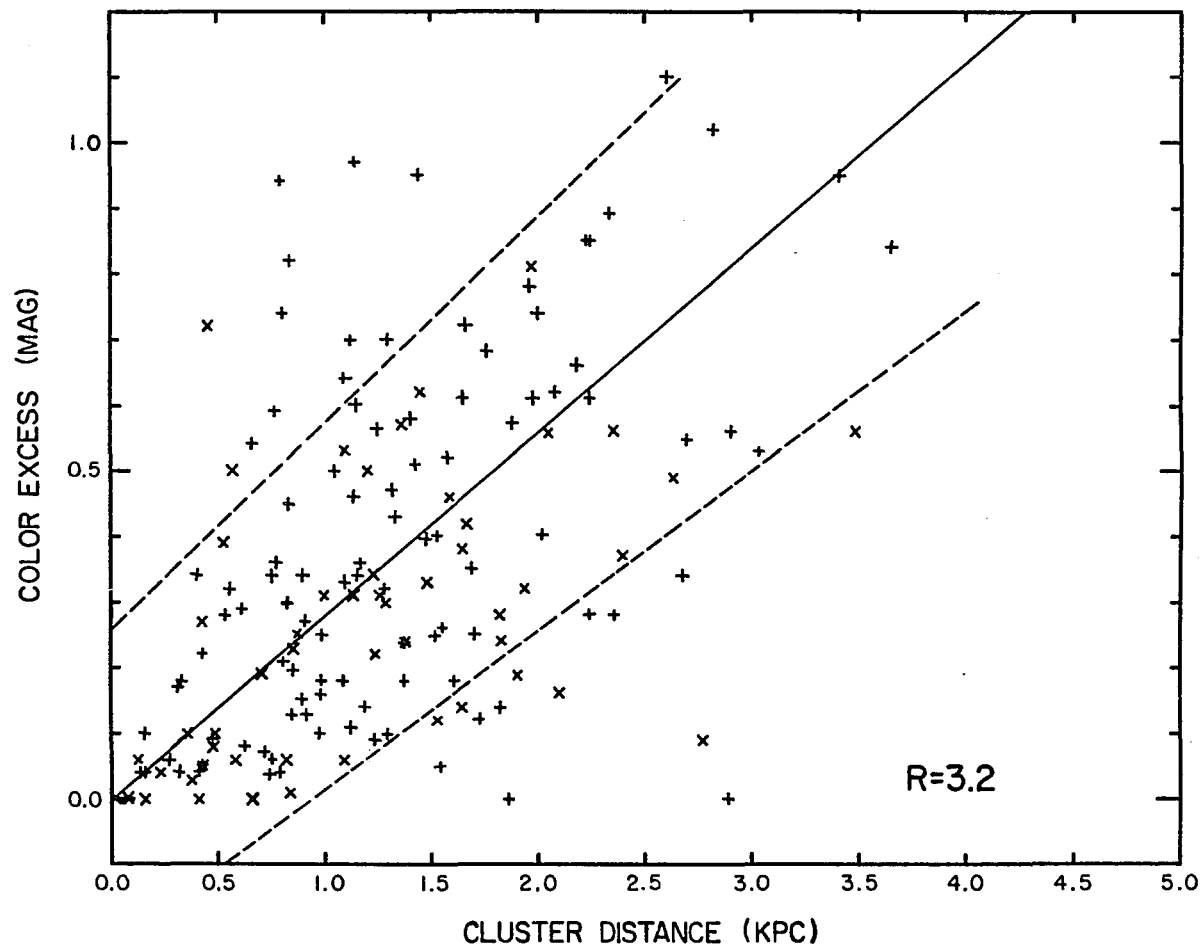


Figure 10. E_{BV} as function of cluster distance ($R = 3.2$).

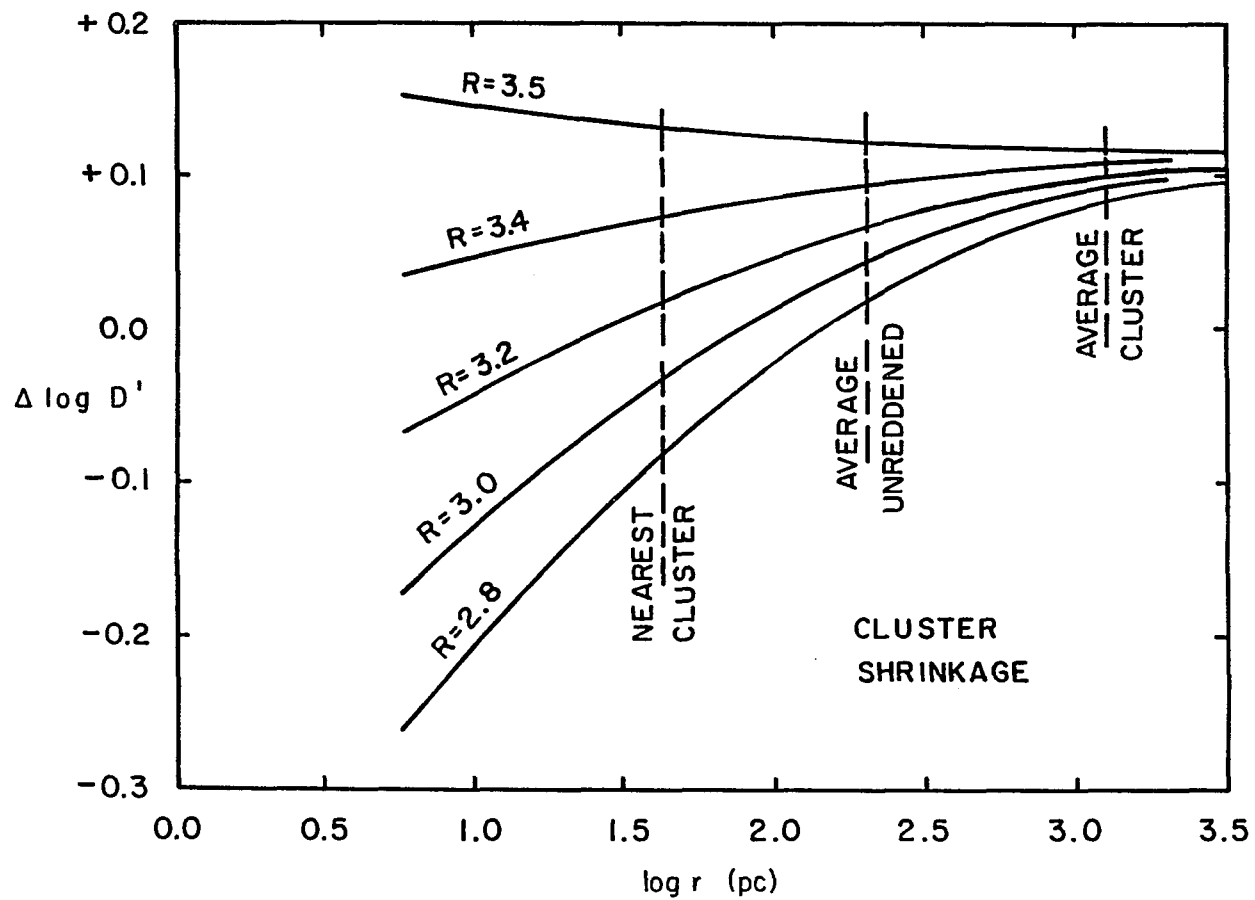


Figure 11. Distance dependent cluster shrinkage with reddening for various R values.

shrinkage. The distances shown for the average cluster and the average unreddened cluster were computed using the mean reddening with distance given above. Note that for $R > 3.5$, the reddening caused cluster shrinkage, $\Delta \log D'$, decreases with distance and E_{BV} while for $R < 2.8$, the shrinkage $\Delta \log D'$ is significantly negative for nearby clusters.

I shall assume that clusters do shrink slightly with reddening. This may be explained as the effect of extinction on the relatively faint stars near the cluster boundary. The diminished brightness of these stars reduces the apparent cluster diameter. If the cluster shrinkage is a smooth function of color excess only, then clusters cannot expand with distance and reddening, nor can nearby clusters be significantly larger than the mean unreddened clusters. Consequently, we must have $2.8 \leq \bar{R} \leq 3.5$.

The shrinkage curves are uncertain by about 0.017 in $\Delta \log D'$. Thus only the curves for $\bar{R} \leq 3.0$ have significant curvature. Symmetrically between the limits of \bar{R} is $\bar{R} = 3.15$. A straight line fit to the curve for $\bar{R} = 3.15$ seems the best representation for the shrinkage of all the clusters. Assuming that we can be confident at the ninety-five percent level that $2.8 \leq \bar{R} \leq 3.5$ and that a straight line is representative in the range $2.4 < \log r < 3.5$ (where the statistics are significant), then

$\bar{R} = 3.15 \pm 0.20$. In this case, as color excess is linear with distance, $\Delta \log D' \approx 0.075(\Delta \log E_{BV})$ and $D' \propto E_{BV}^{-0.075}$ (indeed a weak dependence),

Table II presents the final shrinkage corrected mean type residuals and mean linear diameters. The diameter estimates agree in their ratios to $\sigma \approx 10\%$ with the diameter ratios in the smaller sample studied by Lynds (1967). The mean size of the clusters in the present study is systematically 20% smaller than that given by Lynds (1967), probably because of apparent diameter effects and type differences between our samples. A careful study of the residuals remaining after the final type residuals are removed, again shows that there is no measurable variation of R with galactic longitude, distance from the galactic center or spiral arm number. The best mean value remains $\bar{R} = 3.15 \pm 0.20$.

A Measure of Large Particle Extinction

Grey extinction results when particles are large compared to the wavelength of observation (radius $a \gg \lambda$). To obtain a measure of such extinction one can use a geometric method, such as the cluster diameter method, and a photometric method to make estimates of a variable such as R , which is an indicator of the total extinction present ($A_V = RE_{BV}$). Having already established a mean value

TABLE II^aFinal Mean Type Residuals
and Linear Diameters

Type Residuals

	I	II	III	IV
r	+0.13	+0.13	+0.26	+0.44
m	-0.07	0.0	+0.26	+0.28
p	-0.18	-0.18	0.0	+0.16

Linear Diameters

	I	II	III	IV
r	5.33	5.33	7.20	10.9
m	3.36	3.95	7.20	7.5
p	2.60	2.60	3.95	5.7

- a. The mean type residuals are unitless, each being the logarithm of the ratio of the mean cluster diameter of that type to the mean cluster diameter of all types. The units of the mean linear diameters are parsecs.

$\bar{R} = 3.15 \pm 0.20$ by the cluster diameter method, it remains only to obtain a representative average value of R using a photometric method.

A comparison of the variable extinction and color difference methods (e.g., see Chapter I) leads to the conclusion that the color difference method is preferred because it is subject to fewer uncertainties. Color difference determinations describing a variety of galactic regions include: Grubissich (1968) who studied forty early type stars and found R close to 3.0; Lee (1970) who studied 103 M supergiants and found $R \cong 3.3$ (effective λ corrected to 10^4 °K BB); Schultz and Weimer (1975) who studied 350 early type stars and found $R = 3.14 \pm 0.10$; an unpublished analysis by M. de Vries (1972) of 360 early type stars with 2.2μ m measures gave $R = 3.15 \pm 0.25$; and Serkowski et al. (1975) whose values of $5.5\lambda_{\text{max}}$ imply an average $R = 3.0 \pm 0.24$. My reexamination of the color difference photometry of Grubissich (1968), Johnson (1968) and Lee (1970) using the effective wavelength table in the appendix of Lee (1968) results in average values of R of 3.08 ± 0.24 , 3.15 ± 0.15 and 3.21 ± 0.11 respectively. A weighted mean of these is $R = 3.17 \pm 0.05$. Considering the recent work of Schultz

and Weimer (1975), de Vries (1972), and Serkowski et al. (1975) and the earlier mean, it seems a representative value is $\bar{R} = 3.15 \pm 0.05$.

Comparing $\bar{R} = 3.15 \pm 0.20$ from the cluster diameter method with $\bar{R} = 3.15 \pm 0.05$ from the color difference method, it seems that we may be confident that, in general, there is no significant grey attenuation by large particles. A reasonable limit is that at most 7% of A_V is due to particles large compared to $2\mu\text{m}$ (the wavelength conventionally used as the last point on the color difference plot).

CHAPTER III

DESIGN OF THE INSTRUMENT FOR IR OBSERVATIONS

The program of IR observations began with the expectation that the faintest possible sources would be measured with high accuracy between 1 and $4\mu\text{m}$. Our selection of an instrument design was delimited by constraints of pre-existing equipment and established technique (see Low and Rieke 1976). The system design involved mating of the detector Dewar with the Rieke photometer body, the existing control and amplifier electronics and the beam switching driver system on the 154 cm Catalina telescope of the Lunar and Planetary Laboratory. Dr. Rieke designed the InSb detector and preamplifier system after the general outline of Hall et al. (1975). The system was built by Harris and Rieke with the help of Lunar and Planetary Laboratory and Steward Observatory staff and was later, 1976, modified by Rieke and others.

The InSb photovoltaic detector was operated at LN_2 temperature. The system is most effective in the 2- $5\mu\text{m}$ region (reaching peak efficiency near $5\mu\text{m}$). Most of the

IR measures (see Chapter IV) were made in this wavelength range.

Conventional IR measurement techniques were used (Low and Rieke 1976), including beam-switching background compensation in R.A. at 20 Hz. The detector was used with a beam size of 11.4 arc seconds on the 154 cm Catalina telescope and 8.5 arc seconds on the Steward Observatory 2.3 meter telescope with beam separations of 15 and 9 arc seconds respectively.

The distinctive features of the system design are the placement of the filters inside the dewar adjacent to the aperture diaphragms and the selection of the filters (see Table III). With the filters inside the dewar on a filter wheel, the system background noise is reduced. Furthermore, by placing the filter wheel immediately in front of the aperture wheel the accuracy of registration from filter to filter was improved. This feature is of special importance to my observing program, where sources were located by carefully maximizing the signal in one photometric band and then switching to another band for color measurements.

Table III lists the wavelengths and FWHM values of the filters used to make the observations reported in Chapter IV. The wavelength data for the filters is at LN_2 temperature.

TABLE III
Filter Characteristics

Name	$\log \lambda_0$	$\lambda_0 (\mu\text{m})$	FWHM(μm)
J	0.097	1.25	0.2
H	0.204	1.60	0.4
2.17	0.3355	2.165	0.18
K	0.342	2.20	0.60
2.3	0.3701	2.345	0.06
3.0	0.4790	3.013	0.08
3.1	0.4925	3.108	0.07
3.4	0.534	3.420	0.16
L	0.554	3.58	1.01
3.8	0.582	3.82	0.51

Magnitude measures with this system have, for secondary standards and for program stars with multiple measures, a precision (see Table V) of ± 0.01 mag for sources as faint as $K = 9$ (mag). Consequently magnitudes have been given to three decimal places, although the last figure is generally of marginal significance. Upon careful analysis the observations made with the present system show that near and mid IR ($1-4\mu\text{m}$) photometric observations of bright stars can be made with a reproducible accuracy comparable to UBV photometry.

CHAPTER IV

INFRARED OBSERVATIONS OF A HEAVILY OBSCURED REGION SHOWING PECULIAR EXTINCTION

Introduction

The abnormally high values of R and the large λ_{max} of polarization found in certain dense interstellar clouds, most notably the very dense cloud south of ρ Oph (Carrasco et al. 1973; Strom, Strom, and Carrasco 1974; Strom et al. 1975; Vrba et al. 1975 and Grasdalen et al. 1975), have been used to argue for the presence of larger than normal particles resulting from the action of grain growth. The interstellar diffuse bands in such regions seem to have a reduced strength relative to the continuum opacity, further suggesting the action of grain growth (Snow and Cohen 1974). Theoretical discussions have repeatedly pointed to water ice as the most likely grain growth material, a material which readily condenses out of cold interstellar gas (Greenberg 1968). Water ice is therefore the prime candidate grain growth material.

Using photometric measurements I have determined the relative ice abundance and the relation of that abundance to conditions in the Ophiuchus dark cloud, Analysis of the

photometry establishes the shape of the IR extinction curve, an indication of the grain size, and the absorption strength of the water ice OH stretch band at $3.1\mu\text{m}$ (the most conveniently placed ice absorption in the interstellar extinction spectrum). Furthermore, the measurements show that there is a relation between the onset of ice condensation and the density of interstellar matter (see Chapter V); a relation which is consistent with and significantly extends the conclusions of previous studies (Danielson, Woolf, and Gaustad 1965, Knacke, Cudaback, and Gaustad 1969; Gaustad et al. 1969; Gillett and Forrest 1973; Merrill and Soifer 1974; and Gillett et al. 1975).

Observations

As discussed in Chapter III, our observations were made using conventional IR measurement techniques. The observations were primarily made with the 154 cm telescope of the Catalina Observatory, Lunar and Planetary Laboratory, during the spring of 1975 and 1976, by D. H. Harris and Dr. G. Rieke. Atmospheric extinction coefficients for each night of observation were computed from magnitude and color difference observations of the standard and comparison stars. These coefficients were then used in computing the program star K magnitudes relative to the standard stars

and the program star colors relative to the comparison stars. For those sources where there was no visible star, repeated measures with the K filter normalized the measures with other filters, yielding the measures needed to give a complete set of $(K - \lambda)$ colors and K magnitudes for all stars measured.

Table IV lists the magnitudes of the standard and comparison stars. The zero point of the magnitude system is set by the standard stars α Boo, α Vir, α Lyr and β Lib whose magnitudes are taken from Johnson et al. (1966). The weakly reddened stars δ Sco and 22 Sco are secondary standards for the Ophiuchus region. Each was measured with high precision ($\sigma = 0.01$ mag) on three nights with full atmospheric extinction transforms relative to different sets of primary standards. These two stars are also the principal comparison stars for the Ophiuchus region, their colors having been determined using the optical region photometry and spectral types from Garrison (1967), our IR photometry, and a model extinction curve. All the comparison stars are early type dwarf stars selected for their minimal reddening and proximity to the program stars, and carefully measured relative to the standard stars. In all cases the comparison star colors have a measured accuracy $\sigma \leq 0.01$ mag.

TABLE IV
Magnitudes of Standard
and Comparison Stars

Star Name	J	H	K	L	Code ^a
α Boo			-3.00	-3.14	(1)
α Vir			1.68	1.67	(1)
α Lyr			0.02	-0.02	(2)
β Lib			2.86		(2)
δ Sco	2.58	2.61	2.71	2.66	(2)
22 Sco	5.04	5.08	5.15	5.10	(2)
BS 7769			(5.49)		(3)
BS 7826			(5.42)		(3)
BS 8677			(6.19)		(3)

- a. Code indicates the type of usage of the star.
- Code (1) stars are absolute standards used only to set the zero point of the magnitude system.
- Code (2) stars are used both as zero point standards and color difference comparison stars.
- Code (3) stars are used for color comparison only. (Magnitudes of Code 3 stars are our measures.)

Table V presents the IR photometry of our program stars out to $3.8\mu\text{m}$, the result of combining the K magnitudes and $(K - \lambda)$ colors. The program star $(K - \lambda)$ colors were obtained by directly comparing measures of program stars with measures of comparison stars at nearly equal air mass. Measures of the stars VI Cyg 12 (Cyg OB 2 No. 12) and HD 168607 were made in order to determine the ice band strength and extinction curve shape for stars obscured mostly by dust in the general interstellar medium. In the dense dust cloud south of ρ Oph our photometry is generally at positions determined by coordinate offsets from the visible stars HD 147889, SR 3 or 22 Sco. The scatter in our measures of magnitudes and colors from night to night through 1975 and 1976 and between observers was within the expected range of photometric uncertainty and showed no evidence for the variability of the observed stars. However, since some of the fainter stars were measured on only one or two nights, variability may have been missed in one or more instances. Presuming no variability, the tabulated measures are weighted means. In the wavelength interval 2.1 to $3.8\mu\text{m}$ the accuracies of the color measures are generally much better than the tabulated K magnitude uncertainties. The non-statistical uncertainties in color are generally about 0.01 mag for

TABLE V^a
Magnitudes of Program Stars

Ophiuchus Region

Name\Filter	J	H	2.165	K	2.345	3.013	3.108	3.42	L ^b	3.82	Ref.
HD 147889	5.301	4.856	4.582	±.013							
				4.564	4.523	4.421	4.416	4.335	4.301	4.288	(1)
				±.05					±.05		(2)
	5.28	4.80		4.60					4.42		(2)
				4.52					4.38		(3)
				±.006							
SR 3 ^c	7.679	6.970	6.536	6.491	6.438	6.232	6.202	6.107	6.067	5.977	(1)
				±.05					±.05		(2)
				6.47					6.41		
GS 31 ^d	8.920	7.404	6.750	±.010							
				6.683	6.537	5.868	5.801	5.507	5.365	5.213	(1)
				±.12	±.10				±.15		
				8.883	7.380				5.56		(4)
	11.42	9.35		7.26					5.73		(5)
GS 32 ^d	10.892	8.502	7.131	±.014							
				7.053	6.838	6.034	5.885	5.535	5.321		(1)
	>11.47	8.15		6.64					4.93		(5)
GS 26 ^d	±.13	14.04	11.136	±.02		±.05					
				8.984	8.690	7.790		7.10	(6.89)		(1)
	≥12.08	10.55		8.88					6.88		(5)
VS 18 ^e	±.30	±.04	15.19	±.02	±.02	±.04		±.05			
				9.79	9.502	9.375		8.05	(7.90)		(1)
				≥13.17	10.27						(5)
GS 30 ^d	±.30	14.56	10.81	±.02		±.06					
				8.13	7.87	7.41		6.31	(6.12)		(1)
				7.74					6.73		(5)

TABLE V Continued

Name\Filter	J	H	2.165	K	2.345	3.013	3.108	3.42	L	3.82	Ref.
VS 17 ^e	+ .6										
	- .4	± .03		± .012							
	15.69	11.90	8.955	8.845	8.434	7.930	7.799	6.468	6.224	5.833	(1)
		11.33		8.54					6.64		(5)
VS 26 ^e	+ .6					+ .4					
	- .4			± .02		- .3			± .03		
		15.04		10.51		11.39			8.07		(1)
		10.83		9.12					7.79		(5)
<u>Other Program Stars</u>											
HO 168607				± .01							
			3.403	3.345	3.289	3.072	3.010	2.905	2.881		(1)
VI Cyg 12				± .02							
			2.744	2.715	2.635	2.405	2.375	2.281	2.217	2.178	(1)

a. References for the photometry are:

- (1) D. H. Harris and Dr. G. Rieke for the present work.
- (2) Carrasco et al. (1973)
- (3) Breda, Glass and Whittet (1974)
- (4) Rydgren, Strom and Strom (1976)
- (5) Vrba et al. (1975)

b. The numbers in parentheses are computed from the same polynomial fits (to our photometry, generally from 1.6 to 3.4 μ m) which are used in computing the continuum level at the wavelength of the ice band.

TABLE V Continued

-
- c. The designation SR 3 is from the slit spectrum survey of Struve and Rudkjøbing (1949). This designation is used in the 2 μ m survey paper of Grasdalen, Strom and Strom (1973), it is used by Carrasco, et al. (1973), and by Verba et al (1975).
 - d. The GS numbers are entry numbers in the Table 1 of Grasdalen et al, (1973) where the source coordinates are specified.
 - e. The VS numbers specify sources in Table 1 of Vrba et al, (1975). The Vrba et al. photometry of GS 26, GS 30, GS 31 and GS 32 is according to their Table 2. However, comparing coordinates for those GS sources with VS designations reveals several designation errors, bringing into question the identifications of the VS sources and perhaps partially explaining the discrepancies with our photometry.

the brighter sources, increasing to 0.03 mag for the faintest sources. Statistical errors are given whenever they exceed a few percent. All the tabulated magnitudes are effectively monochromatic, having been corrected for filter width effects using the formulae of King (1952). Since the magnitudes given by other authors have the same corrections as our measures, their measures may be directly compared with ours.

Our observations of GS 31 agree well with those of Rydgren, Strom, and Strom (1976). Our observations also agree reasonably well with those of Carrasco et al. (1973), our measures of δ Sco agree with Johnson et al. (1966), our measures of HD 147889 agree with Breda et al. (1974), and our measures of VI Cyg 12 agree with previous values given by Voelcker (1975) and by Gillett et al. (1975). However, comparing our measures with those of Vrba et al. (1975) reveals discrepancies of more than a magnitude in several instances. We have no explanation for these discrepancies, but we wish to emphasize that the repeatability and signal-to-noise of our measurements indicate errors of no more than a few percent (except where larger errors are indicated in Table V).

Table VI lists the available optical region photometry, color excesses and spectral types for the sources

TABLE VI*

Color Excesses of Stars with Optical Photometry

Star Name	V	Sp	E _{BV}	E _{VR}	E _{VJ}	E _{VH}	E _{VK}	E _{VL}	A _V
HD 147889 ^a	± 0.02 7.90 ^b	B2 V ^c	± 0.04 1.09 ^b	(1.03) ¹	3.14	3.68	4.05	4.28	4.50
SR 3 ^d	12.00 ^e	B8 V ^f	± 0.08 1.42 ^g	(1.49) ¹	4.50	5.23	5.75	6.15	6.40
HD 168607 ^h	8.29 ⁱ	B9 Ia ⁺ _p ¹	± 0.03 1.60 ⁱ	(1.48) ¹	(3.87) ¹	(4.43) ¹	4.91	5.35	5.65
VI Cyg 12 ^j	11.48 ^k	B8 Ia ^k	± 0.03 3.24 ^k	3.17	7.10	8.17	8.80	9.27	9.65

* The IR color excesses are probably uncertain by ~ 0.1 mag because of uncertainties in spectral type and intrinsic colors.

- a. The IR photometry of HD 147889 is by Harris and Rieke for the present work. Photometry by Serkowski (1968) and by Breda et al. (1974) generally agrees with ours within their given error estimates.
- b. The V magnitude and E_{BV} of HD 147889 are weighted mean values from Hiltner (1956); Hardie and Crawford (1961); Serkowski, Gehrels and Wisniewski (1969); Coyne, Gehrels and Serkowski (1974); Serkowski et al. (1975); and Breda et al. (1974).
- c. The spectral type of HD 147889 is uniformly described as B2 V by Hiltner (1956), Garrison (1967) and in recent works which may rely on the Hiltner and Garrison types.
- d. The IR photometry of SR 3 is by Harris and Rieke for the present work.

TABLE VI Continued

-
- e. The V magnitude of SR 3 is from Carrasco et al. (1973),
 - f. The spectral type is an average of the value given by Struve and Rudkjøbing (1949) and our estimate from the star's absolute magnitude (see Table IX).
 - g. The E_{BV} of SR 3 uses the (B-V) color of Carrasco et al. (1973), the spectral type from column 3 and the intrinsic colors from Johnson (1968).
 - h. The IR photometry of HD 168607 is by Harris and Rieke for the present work.
 - i. The optical photometry and spectral type of HD 168607 are from Hiltner (1956).
 - j. For VI Cyg 12 (Cyg OB 2 No. 12) the R, J and H photometry are weighted means from values given in Voelcker (1975) and the K and L photometry is from the present work.
 - k. The optical photometry and spectral type of VI Cyg 12 are from Johnson (1968).
 - l. Except for VI Cyg 12 the E_{VR} values are obtained using interpolation in Figure 12, consequently those excess values are given in parentheses, as are the similarly estimated J and H excess values for HD 168607.

we have measured. The values of A_V are estimated by extrapolation from the extinction curves in Figure 12. There is some uncertainty in the spectral types and therefore the intrinsic colors of these stars, particularly VI Cyg 12 (Chaldu, Honeycutt, and Penston 1973) and SR 3 (Struve and Rudkjøbing 1949). At the low dispersion used to study SR 3, its faintness and strong reddening may have biased its classification. I suspect an earlier spectral type (see below). However, in most cases the spectral type uncertainties should not seriously affect the computed excess ratios.

The Extinction Curves

Table VII and Figure 12 present the color excess ratios and extinction curves of the program stars with accurate optical region photometry. All the color excesses in Table VII and Figure 12 are from Table VI. Since there is no J or H photometry of HD 168607, the values of $\frac{E_{VJ}}{E_{BV}}$ and $\frac{E_{VH}}{E_{BV}}$ are obtained by interpolation from Figure 12 and are therefore in parentheses. The values of R are extrapolations using the extinction curves in Figure 12. Intrinsic color uncertainty is the major source of uncertainty in the excess ratios. Total uncertainties

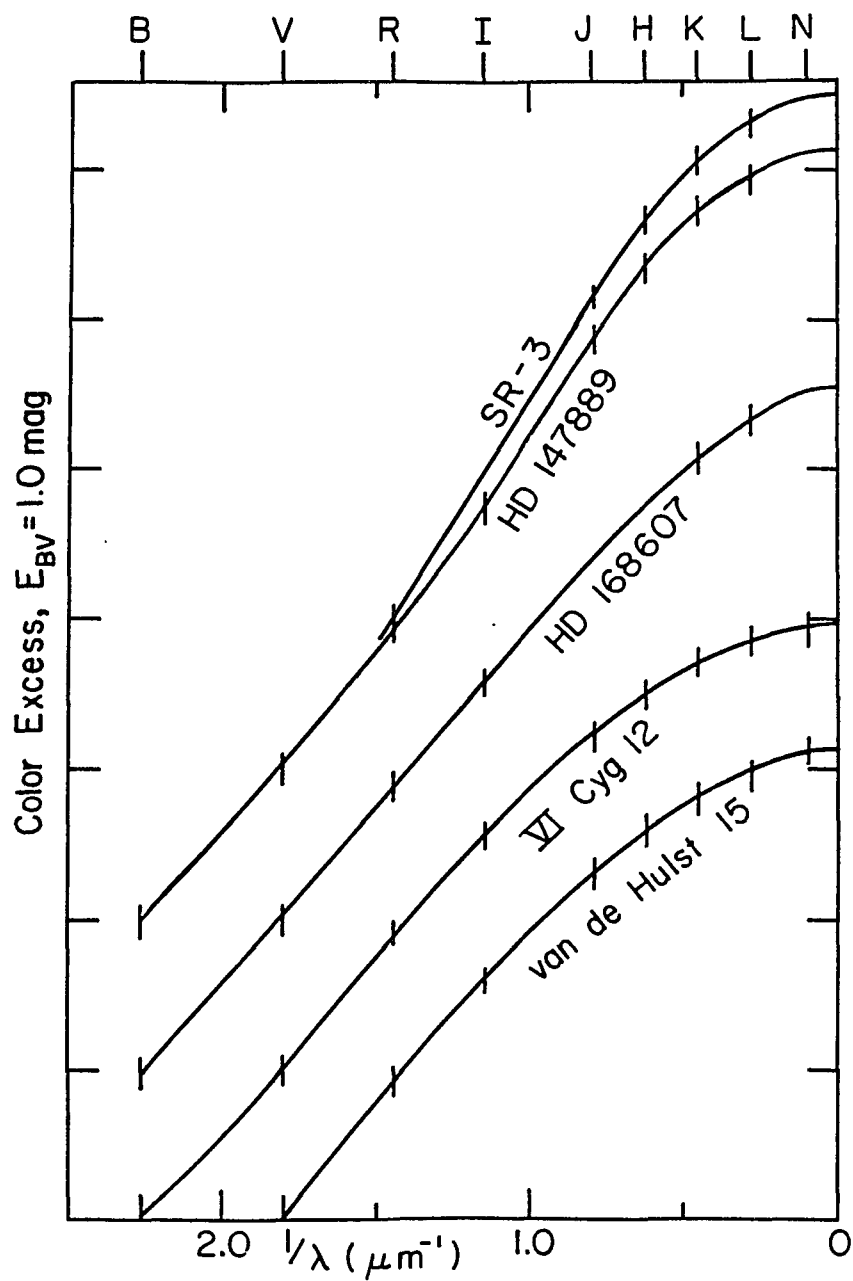


Figure 12. The extinction curves for stars with optical region photometry and van de Hulst 15.

TABLE VII
Color Excess Ratios of Stars
with Optical Photometry

Star Name	$\frac{E_{VJ}}{E_{BV}}$	$\frac{E_{VH}}{E_{BV}}$	$\frac{E_{VK}}{E_{BV}}$	$\frac{E_{VL}}{E_{BV}}$	R
	$\pm .15$	$\pm .17$	$\pm .20$	$\pm .20$	$\pm .25$
HD 147889	2.88	3.38	3.72	3.94	4.13
	$\pm .20$	$\pm .25$	$\pm .30$	$\pm .30$	$\pm .35$
SR 3	3.17	3.70	4.07	4.35	4.51
			$\pm .12$	$\pm .13$	$\pm .15$
HD 168607	(2.42)	(2.77)	3.07	3.35	3.53
			$\pm .05$	$\pm .05$	$\pm .07$
VI Cyg 12	2.19	2.53	2.72	2.86	2.98
v de H 15	2.29	2.58	2.82	2.99	3.14

are generally between 2 and 6%. The classical theoretical extinction curve, van de Hulst No. 15, is included in Table VII and Figure 12 for convenient comparison (Lee 1968). For VI Cyg 12 I have additionally plotted the N measure from Rieke (1974). Since the IR photometry of VI Cyg 12, from the compilation of Voelcker (1975), gives a very bumpy extinction curve, (deviations from a smooth curve amount to ~ 0.1 mag) I have plotted a smoothed extinction curve. The extinction curves are extrapolated from the longest available wavelength to $1/\lambda = 0$ using the constraint that near $1/\lambda = 0$ the slope is zero. It is noteworthy that in Table VII the values of R for the two visible stars in Ophiuchus are nearly equal at $R = 4.3$,

in agreement with the variable extinction analysis of stars in this region by Whittet (1974). The R values are also consistent with those found by Carrasco et al. (1973).

For the heavily obscured sources in the Ophiuchus cloud it was necessary to assume that our observations are of the heavily obscured photospheres of stars. Arguments for this assumption are given below.

There is little doubt that the upper Scorpius region including the region around ρ Oph has been the site of a recent episode of intensive star formation. This can be seen from the large number density of visible early type stars and $H\alpha$ emission sources, (Carrasco et al. 1973, Struve and Rudkjøbing 1949); and the star density excess noted by Bok (1956). Carrasco et al. (1973) estimate the cluster's age at about 10^7 years. This region can be best described as a newly formed open cluster still embedded in dense cold gas and dust from which it formed. It therefore seems quite reasonable that the IR sources are heavily obscured early type stars.

Our initial IR color excess ratios were computed assuming that all the sources are A0 V type stars. Fortunately, these ratios are not sensitive to the exact spectral type chosen. The similarity of the resulting IR extinction curves (see Table X and Figure 13) supports the

contention that the sources are heavily obscured stars. Using these first-generation extinction curves, I then estimated the unreddened magnitudes of the sources. In order to compute the absolute magnitudes of the IR stars it is necessary to assume that they are all at approximately the same distance as the visible stars and dust. That assumption is supported by our finding of associated emission excesses for the stars thus far measured out of $10\mu\text{m}$. See Table VIII. These observations suggest that the stars are surrounded by dust shells. With all the sources at the distance modulus of the association, $(m - M) = 6.0$ (Jones 1970; Galspey 1971; Walborn 1972; and Whittet 1974), their absolute magnitudes range between about -3 and $+1$, showing that they are most likely either B or A type dwarfs; G, K or M type giants or luminosity class II stars (Blaauw 1963). The normal spectral type - absolute magnitude diagram of a young open cluster shows that most of the stars with $1 \geq M_V \geq -3$ are on the main sequence, a few are giants, and it is extremely rare to find a luminosity class II star.

Very long wavelength studies of the ρ Oph region put an upper limit on the temperatures of the embedded stars. The radio continuum and recombination line data, and the microwave molecular emission observations show that

TABLE VIII ^a

Magnitudes of Ophiuchus Stars
Having Far IR Photometry

Name	K	L	5 μ m	10 μ m	10.4 μ m	10.6 μ m
GS 31	$\pm.01$ 6.68	$\pm.02$ 5.37	$\pm.15$ 5.38	$\pm.10$ 3.05		
GS 30	$\pm.02$ 8.13	$\pm.03$ (6.25)	$\pm.10$ 4.60		$\pm.05$ 1.67	$\pm.05$ 1.63
VS 17	$\pm.01$ 8.85	$\pm.02$ 6.22	$\pm.06$ 4.67		$\pm.11$ 3.69	$\pm.05$ 3.51

- a. All K and L photometry is from Table V. For GS 31 the far IR photometry is from Rydgren et al. (1976). The remainder of the far IR photometry is by Rieke (for the present work). Tabulated errors are statistical errors. The 5 μ m and 10 μ m measures of Rydgren et al. (1976) are with broad band filters. The 10.4 μ m and 10.6 μ m filters are 1.3 μ m and 5 μ m wide respectively. Only the K and L magnitudes are monochromatic. However, the filter width corrections are small compared to the far IR emission excesses.

the gas within the cloud is mostly neutral, with $(n_e/n) \approx 10^{-5}$ (Brown et al. 1974), except in a few compact H II regions around embedded hot stars; that the gas density is high, $n \approx 10^5 \text{ cm}^{-3}$ (Penzias 1972, Encrenaz 1974, and Brown and Zuckerman 1975); that the gas temperature is about 20°K , which is about a factor of three higher than the temperature in most dark clouds (Heiles 1973, Encrenaz 1974, and Brown et al. 1974) that, for the most part, the dust grain temperature $T_d \sim 50^\circ\text{K}$ (Fazio et al. 1976). The dust temperature is consistent with heating by embedded stars. Also, the velocity dispersion of the radio and microwave lines thus far observed is small, $\Delta v \approx 1.5 \text{ km/sec}$, indicating quiescent conditions in the cloud (Heiles 1973, Brown et al. 1974, and Chaisson 1975). These observations along with measures of the compact H II regions show that none of the stars in this region is earlier than late O spectral type and that the embedded stars responsible for the radio and microwave emission are most likely between B2 V and B8 V spectral type.

Our filter set includes a narrow filter at the $2.31\mu\text{m}$ CO band which should permit us to discriminate between giant and dwarf stars (Frogel et al. 1975). For normal G, K, and M type stars, the $2.31\mu\text{m}$ CO band is strong in luminosity class I, II, and III stars and is

weak or absent in dwarf stars. Stars earlier than G show no CO absorption at all. Our measures give no indication of CO absorption in any of the measured IR stars (see Table V). Considering the usual distribution of spectral types in a young cluster, the radio and microwave data, and the absolute magnitudes; those IR stars with CO measures are probably B or A type dwarf stars. Although we have no CO-band measurement for VS 26, since it has no apparent photometric abnormality I have assumed that it also is an early type dwarf star.

With the IR sources tentatively classified as early type dwarfs, I estimated their spectral types from their computed absolute magnitudes and used the intrinsic colors of the estimated spectral types to compute a revised set of color excess ratios. Table IX gives the computed absolute magnitudes and estimated spectral types of the Ophiuchus stars. For HD 147889 comparison with the known spectral type shows good agreement, giving confidence in the estimated spectral types. But for SR 3 the estimated spectral type is B6, whereas Struve and Rudkjøbing (1949) give A0. Considering the expected bias in their classification due to low dispersion and strong reddening, I have computed the color excess assuming a B8 V spectral type. The stars GS 31 and GS 32 both show

TABLE IX
De-Reddened Magnitudes and Estimated
Spectral Types of Ophiuchus Stars

Name	Sp	M_V (± 0.6) (mag)
HD 147889	B2 V	-2.5
SR 3	B6 V	-0.5
GS 31	B5 V	-1.0
[GS 31] ^a	K5 III	+3.5]
GS 32	B4 V	-1.5
[GS 32] ^b	M0 III	+3.0]
GS 26	B6 V	-0.5
VS 18	B8 V	0.0
GS 30	B2 V	-2.5
VS 17	B3 V	-2.0
VS 26	B2 V	-2.5

- a. Intrinsic colors are from Johnson (1964).
b. Intrinsic colors are from Lee (1970).

peculiar color excess ratios if they are assumed to be early type stars (see Table X). Again considering the available evidence, it was recognized that these stars might be late type giants or protostars, peculiarly lacking CO absorption. Therefore Table IX includes late type models of these stars.

Table X and Figure 13 present the measured color excess ratios and average extinction curves normalized to $E_{HK} = 1$. The excess ratios were normalized to E_{HK} because it is accurately measured for all the Ophiuchus stars and should not be affected by circumstellar emission. Magnitudes at R of 14.3 ± 0.4 for GS 31 and 18.5 ± 0.5 for GS 32 were measured on the Palomar Observatory Sky Survey prints by comparison with a calibrated sequence of red print magnitudes. All other magnitudes used in computing the color excess ratios in Ophiuchus are taken from the measures listed in Tables V and VI. In order to estimate the E_{VK} values for GS 31 and GS 32, and to estimate other excesses for the heavily obscured stars, it was necessary to use average color excess ratios. Since, for both HD 147889 and SR 3, our measures show that $E_{VK}/E_{RK} = 1.35$ (a value not far off the mean of VI Cyg 12 and HD 168607), I have assumed this ratio is constant in the Ophiuchus region and applied it to

TABLE X
Extinction and Color Excess Ratios

Name	Sp	E_{HK}	E_{VK}	A_V	$\frac{E_{VK}}{E_{HK}}$	$\frac{E_{RK}}{E_{HK}}$	$\frac{E_{JK}}{E_{HK}}$	$\frac{E_{KL}}{E_{HK}}$	ΔL (mag)
HD 147889	B2 V	0.37	4.05	4.5	10.9	(8.1)	$\pm .20$ 2.46	$\pm .10$ 0.62	± 0.1 0.0
SR 3	B8 V	0.52	5.75	6.4	11.1	(8.2)	$\pm .20$ 2.40	$\pm .10$ 0.77	± 0.1 0.0
GS 31	B5 V	0.78	(10.8)	(11.8)	(13.9)	$\pm .5$ 10.3	$\pm .1$ 3.01	$\pm .1$ 1.67	± 0.2 0.7
	[K5 III	0.49	(7.1)	(7.8)	(12.0)	$\pm .5$ 8.9	$\pm .1$ 2.27	$\pm .1$ 2.49	± 0.2 1.0]
GS 32	B4 V	1.52	(16.0)	(18.0)	(10.5)	$\pm .5$ 7.8	$\pm .1$ 2.61	$\pm .1$ 1.13	± 0.2 0.6
	[M0 III	1.28	(11.6)	(13.3)	(9.1)	$\pm .5$ 7.0	$\pm .1$ 2.25	$\pm .1$ 1.47	± 0.2 0.9]
GS 26	B6 V	2.21	(23.4)	(26.3)	(10.6)	(7.8)	$\pm .12$ 2.34	$\pm .03$ 0.94	± 0.2 0.4
VS 18	B8 V	2.44	(24.7)	(27.9)	(10.1)	(7.5)	$\pm .17$ 2.24	$\pm .03$ 0.77	± 0.2 0.0
GS 30	B2 V	2.76	(30.0)	(33.5)	(10.9)	(8.0)	$\pm .15$ 2.40	$\pm .03$ 0.72	± 0.2 0.0
VS 17	B3 V	3.13	(31.7)	(35.8)	(10.1)	(7.5)	$\pm .20$ 2.24	$\pm .02$ 0.83	± 0.3 0.3
VS 26	B2 V	4.61	(48.0)	(53.9)	(10.4)	(7.7)	$\pm .10$ (2.30)	0.53	± 0.5 0.0
VI Cyg 12	B8 Ia	3.24	8.80	9.65	11.7	7.8	2.3	0.64	± 0.3 0.0
HD 168607	B9 Ia ⁺ _p	0.49	4.91	5.65	(10)	(7.0)	(2.1)	(0.90)	± 0.1 0.1
v de H 15					13	8.4	2.3	0.77	

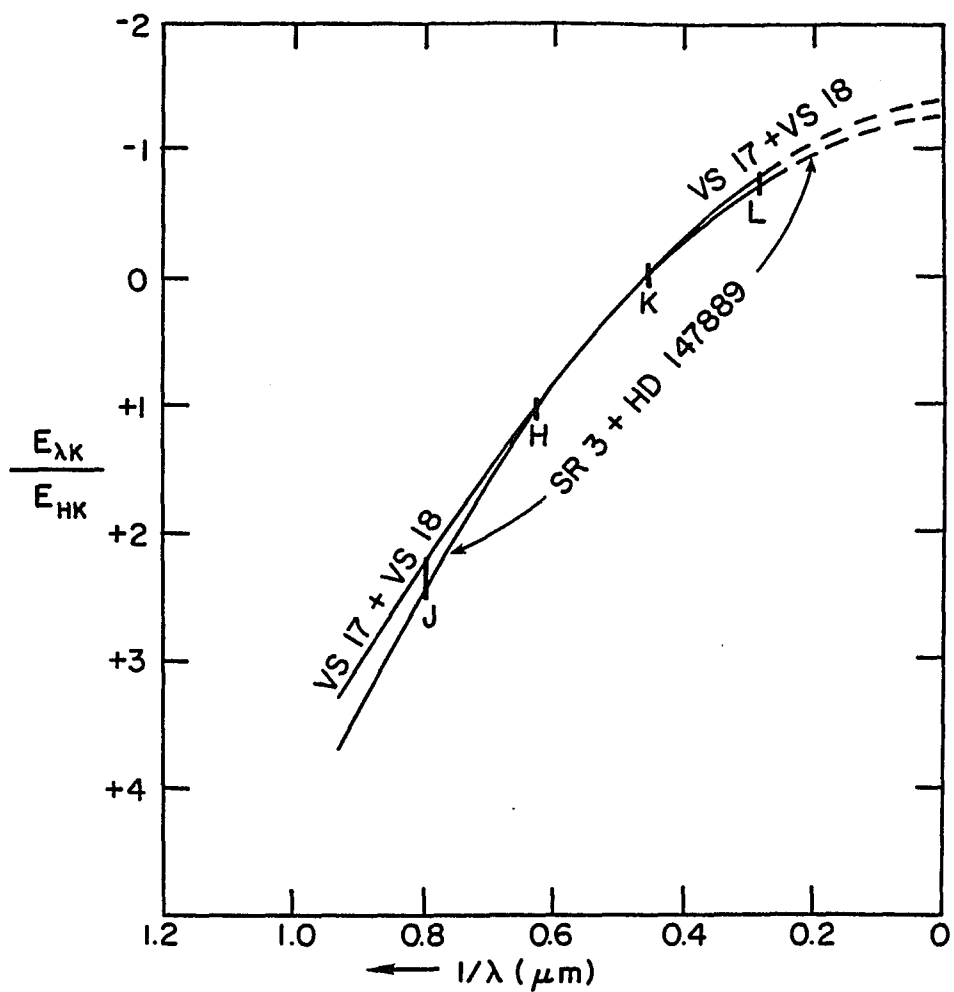


Figure 13. The mean Ophiuchus extinction curves in the infrared.

computing E_{VK} for the other stars. To find E_{RK} and thence E_{VK} for the more heavily obscured stars I used the relation $E_{RK}/E_{JK} = 3.35$ which seems to be a representative value for the Ophiuchus region and not far off of that found elsewhere. For VS 26 which has no J measure I assumed $E_{JK}/E_{HK} = 2.30$, the average value of the ratio for the other heavily obscured stars. The extinction beyond the K filter was estimated using the mean extrapolated extinction curve. I assumed $E_{K\infty} = 1.30E_{HK}$. The estimated circumstellar emission ΔL (mag) is obtained by assuming that normal extinction gives $E_{KL}/E_{HK} = 0.75$. Because of the crudeness of these estimates and the small variation in curve shape, I have plotted average extinction curves in Figure 13.

Table X shows that both GS 31 and GS 32 show peculiar red and infrared extinction curves if they are assumed to be early type dwarf stars (type determined by absolute magnitude fit). If instead, one assumes that the extinction curve is nearly normal, and estimates the spectral type from the (J to K) colors which result when the mean Ophiuchus extinction is removed, then one finds that these stars resemble subluminescent (See Table IX) K or M giants. Their position in the HR diagram is

suggestive of pre-main sequence objects which would reach the ZAMS as F stars. This identification seems questionable however, since the $5\mu\text{m}$ magnitude of GS 31 indicates an emission excess more like that in keeping with the B5 V model (see Tables VIII, IX and X).

Extinction Curve Interpretations

An examination of the extinction curves in Table X and Figure 13 shows that the lightly obscured stars show optical and near IR slopes larger than would be normal for the general interstellar extinction. Considering also that there is an apparent increase in the ratio of total to selective extinction, R , with obscuration (Carrasco et al. 1973, Figure 2; and my Table VII) it seems that we have persuasive evidence for excess IR extinction due to larger than normal particles. Yet as we will see, these stars show little or no ice band extinction (see Table XII). In the infrared, extinction commonly varies as $(1/\lambda)^4$, a recognized characteristic of small dielectric spheres. The IR source stars with well determined extinction show a dependence closer to $1/\lambda$, suggesting either the admixture of small absorbing particles (radius $a \lesssim 0.1\mu\text{m}$) or larger than normal dielectric particles ($a \sim 0.5\mu\text{m}$). That is, the extinction curve looks like a composite of extinction by "normal" and IR particles. It seems that the Ophiuchus

cloud shows a nearly uniform abnormal extinction regardless of obscuration or ice band strength.

If one assumes all the particles are dielectrics then the published dielectric sphere grain models (Wickramasinghe 1973) yield estimated grain sizes by fitting the extinction curve. Taking the normal ratio of total to selective absorption, $R(\equiv A_V/B_V) \approx 3.2$, and the normal visual region extinction curve, eg. an average of VI Cyg 12 and HD 168607, and fitting to the corresponding properties of the relative extinction efficiency curve, $Q_e(\frac{a}{\lambda}, n) \equiv \sigma/\pi a^2$, where n is the refractive index and $\lambda = \lambda/2\pi$ is the reduced wavelength, shows that in the normal interstellar medium generally $Q_e(\lambda = 0.55\mu\text{m}) \approx 2.6$, and the mean particle radius $\bar{a} \approx (0.11\mu\text{m})/(n-1)$. This size is consistent with similar fits done by Greenberg (1968, p. 310) and by Spitzer (1968, p. 67). A similar fit to the optical extinction in the moderately opaque portions of the Oph cloud, using $R \approx 5.0$, yields $Q_e(\lambda = 0.55\mu\text{m}) \approx 3.2$ and $\bar{a} \approx (0.13\mu\text{m})/(n-1)$. On examining the more general case of Q_e curve fitting for dielectric spheres I found that for $6 \gtrsim R \gtrsim 2.8$, the variation in $Q_e(\lambda = 0.55\mu\text{m})$ with grain size very nearly (to $\sim 6\%$) compensates for the size dependence of the geometric cross section of a constant mass of grains. Fitting this general $Q_e(\frac{a}{\lambda}, n)$ to the optical

extinction in the less obscured regions of the cloud
 $(1 \gtrsim E_{HK} \gtrsim 0.3 \text{ and } 6 > R > 4)$ yields a constant absolute efficiency,

$$\xi(\lambda = 0.55\mu\text{m}) \equiv \frac{\pi a^2 Q_e}{\frac{4\pi a^3}{3}\rho} = \frac{3Q_e}{4a\rho} \approx 1.8 \times 10^5 \left(\frac{n-1}{\rho}\right) \text{cm}^2/\text{gm},$$

where ρ is the grain density (gm/cm^3).

Those Ophiuchus stars with well defined extinction curves show nearly linear extinction curves over a factor of two range in $1/\lambda$ centered at $\sim 1.5\mu\text{m}$ (when the emission excess at L is removed). The relative extinction efficiency $Q_e(\frac{a}{\lambda}(n-1))$ for the general dielectric sphere is nearly linear over a range of three in $1/\lambda$ centered at $\frac{a}{\lambda}(n-1) \approx 1.1$. Using the monodisperse approximation, I matched the Q_e curve to the linear IR extinction yielding $\frac{2\pi a(n-1)}{1.5} \approx 1.1$, or $a \approx (0.26\mu\text{m})/(n-1)$. For such grains $Q_e(\lambda = 0.55\mu\text{m}) \approx 2.8$, so $\xi(0.55\mu\text{m}) \approx 8.0 \times 10^4 \left(\frac{n-1}{\rho}\right) \text{cm}^2/\text{gm}$. The combined errors of observation and Q_e fit modeling make the estimated particle radius uncertain by about 30%. The extinction efficiencies are uncertain by a similar amount. If the grain refractive index is constant in the cloud, then the dielectric model grain for the more heavily obscured regions is about 2.2 times the size of the

dielectric model particle in the less opaque regions (volume ratio is ~ 10 to 1), demonstrating that there is a substantial grain size increase upon probing the more opaque regions of the cloud, and suggesting the action of a grain growth process.

Posit that the IR extinction particles are absorbing particles, then because all Rayleigh absorbers (with effectively constant refractive index) show a $1/\lambda$ extinction dependence, the size of the absorbing particles can't be determined. One can only set an upper limit on the particle size. For absorbing particles ($k \gtrsim 0.2$, $m = n - ik$) the upper limit on size for extinction dominated by absorption, and therefore for linear extinction, is $(a/\lambda) \lesssim 1.05/|m-1|$. Assuming the extinction is linear out to $(1/\lambda) \approx 0.9\mu\text{m}^{-1}$ and that $|m-1| \gtrsim 3$, then $a \lesssim 0.06\mu\text{m}$. With this limitation, the increasing relative strength of the IR extinction with increasing obscuration tells us only that the total volume of absorbing grains along our line of sight is increasing, without saying anything about the grain size distribution. Furthermore, for such an absorbing material, without accurate knowledge of the complex refractive index $m(\lambda)$ even the volume of grains is indeterminate.

The Ice Band Extinction Measures

So that the response of our filter-photometer system to ice band extinction would be unambiguous, our program began measuring the ice extinction with two narrow filters. Their response curves measured at LN_2 temperature are each nearly symmetrical, peaking at $3.013\mu\text{m}$ and at $3.108\mu\text{m}$. To determine the response of these filters to ice band extinction I examined the spectra of astronomical sources and compared them with selected laboratory spectral data. Table XI presents a data summary of available astronomical ice band spectra and data for SS Vir (Sp is C6) which has a $3.07\mu\text{m}$ band that is probably not due to ice. There seem to be no significant differences in the ice band profiles between astronomical sources. The profiles are nearly symmetric, being only slightly steeper on the long wavelength side, with a maximum absorption near $3.07\mu\text{m}$ and a FWHM corrected for instrumental broadening of $\sim 0.27\mu\text{m}$.

An examination of the various laboratory spectral studies of H_2O ice by Sill (1976), by Schaaf and Williams (1973), by Bertie, Labbé and Whalley (1969), and by Irvine and Pollack (1968) shows that the best estimates are $3.07\mu\text{m}$ for the band position and $0.25\mu\text{m}$ for the FWHM. However, these laboratory studies give a distinctive and asymmetrical

TABLE XI^a
Astronomical 3.1 μ m Band Data

Name	$\Delta m(3.07)$	$\lambda(\mu m)$	$\Delta\lambda(\mu m)$ FWHM	Reference
BN	1.52	3.07	0.23	Gillett and Forrest (1973)
	1.52	3.08	0.35	Gillett et al. (1975)
	1.59	3.08	0.32	Merrill, Russell and Soifer (1976)
NGC 2024 No. 2	1.03	3.08	0.32	Grasdalen (1974)
	1.25			Merrill et al. (1976)
CRL 2591	1.0	3.08	0.24	Merrill and Soifer (1974)
Rosette Neb. IRS	2.8	3.05	0.28	Cohen (1976)
SS Vir	1.2	3.07	0.27	Merrill and Stein (1976)

- a. Most of the values of $\Delta m(3.07)$, λ and $\Delta\lambda$ are estimates from figures and are thus of low accuracy. The values of $\Delta\lambda$ are generally uncertain by $\sim 0.03\mu m$. [See p. 77 for a definition of $\Delta m(\lambda)$.]

band profile resembling that of hexagonal ice given by Knacke, et al. (1969). In contrast, the nearly symmetrical astronomical band profiles closely resemble the profile of amorphous ice given by Knacke et al. (1969).

The presence of a prominent broad band at $3.07\mu\text{m}$ in little-reddened carbon stars such as SS Vir (Merrill and Stein 1976), and its tentative identification with C_2H_2 in the cool stellar atmosphere, puts the identification of the $3.07\mu\text{m}$ band in some doubt. However, the absence of $2.3\mu\text{m}$ CO absorption in the Ophiuchus IR stars (as well as other arguments) shows that the sources in our sample are probably not carbon stars. The possible presence of an interstellar NH_3 band at $3.0\mu\text{m}$ (Davidson et al. 1972) also causes confusion about the band identification. This situation is further confused by the variable resolution and quality of the astronomical spectra and uncertainties in their wavelength calibrations. Thus it seems that it is not clear when one can identify the $3.07\mu\text{m}$ band with ice alone.

It is necessary at this point to make the theoretical argument that inside ordinary dark clouds (e.g., where $n_{\text{H}_2} \sim 10^5 \text{cm}^{-3}$) the density is far too low to permit the spontaneous nucleation of condensate particles (Watson and Salpeter 1972). Therefore any condensate, including

ice, has to be (alone or in a mixture) in mantles on the grains which were already present in the cloud at the onset of condensation, that is, on core grains.

It was noted by Hulst (1957, p. 193), that the extinction profile of an absorption band depends on the dimensions of the absorbing volume if those dimensions are comparable to the reduced wavelength ($\chi = \lambda/2\pi$). Specifically, for the case of coated grains, if the core grains have small to moderate dimensions then thin enough mantles behave like Rayleigh particles ($a/\chi \ll 1$). Consequently the amount of mantle extinction is independent of the grain geometry and is proportional to mantle volume. Furthermore, the band extinction profile resembles the absorptivity of the bulk mantle material. However, for increasing mantle thickness, the profile becomes progressively more asymmetrical and shifted to longer wavelength (by as much as the band half-width), followed by a dispersion curve shape centered on the normal band wavelength, and ultimately by a pseudo-emission for thick mantles.

The data summarized in Table XI show that the available astronomical ice band profiles resemble the absorptivity profile of bulk amorphous ice (see Knacke et al. 1969). I know of no heavily obscured astronomical source whose $3\mu\text{m}$ spectrum shows a band profile with

substantial asymmetry or pseudo-emission like that expected for moderate or thick mantles. . Therefore it seems reasonable to surmise that in dark clouds there are no grains with thick mantles ($t \gtrsim \lambda$ for the $3.07\mu\text{m}$ ice band). (Further evidence for thin mantles in Ophiuchus is given below.) The apparent validity of the Rayleigh approximation makes it reasonable to combine the astronomical ice band data with the laboratory compromise data to give an estimated ice band extinction spectrum. It should be emphasized that the apparent validity of the Rayleigh approximation also precludes the direct measurement of the thickness of ice mantles. We must be content with estimating an upper limit on mantle thickness.

Figure 14 shows the estimated ice band profile and the positions of our two ice filters. The ice band opacity maximum is at $3.072\mu\text{m}$. The FWHM is $0.25\mu\text{m}$ and the half opacity points are at $2.94\mu\text{m}$ and $3.19\mu\text{m}$. Because of the large breadth of the band, the ice filters should quite effectively measure the band extinction even if the opacity maximum is slightly shifted, e.g., to $3.05\mu\text{m}$.

A further relevant consideration is the possibility that some ice may form a mixture with other molecules or may form a clathrate compound that could modify the position or strength of the ice band (Greenberg 1973). However the

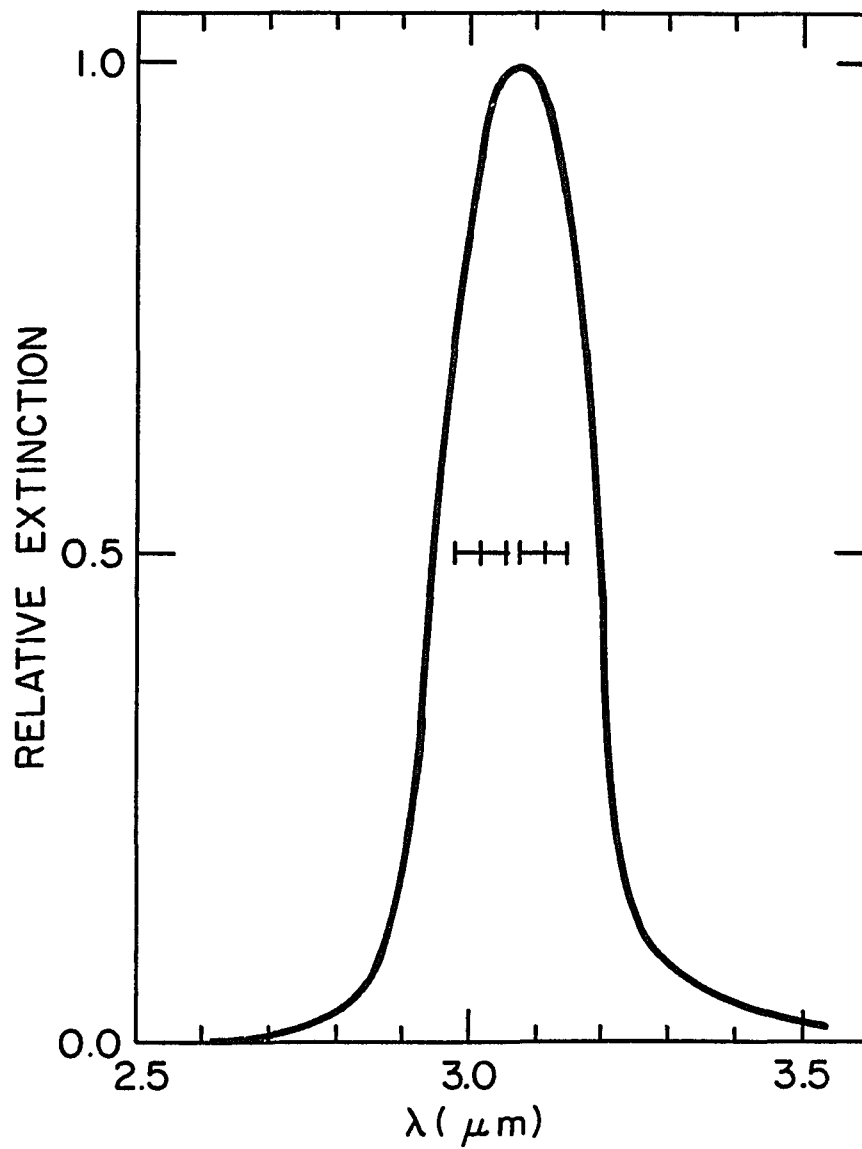


Figure 14. The estimated ice band extinction profile.

work of Hunter and Donn (1971) seems to show that, at least under the conditions of their study, the ice band is unaltered in position or width when the H_2O ice is in a mixture with NH_3 and CH_4 ice. Furthermore, they found no evidence of bondings between the different molecules in the mixture and no dependence of the band profile on the kind of substrate material. In general they found the band profile invariant, with the band strength depending only slightly on the kind of mixture. Unfortunately, Hunter and Donn (1971) do not specify the dependence of band strength on the mixture parameters.

Presuming the band profile is as plotted, the filters should respond to $90 \pm 6\%$ of the peak ice band extinction and their ice band sensitivities should be just about equal. In discussing the band, $\Delta m(\lambda)$ is defined as the extinction in excess of the average adjacent continuum extinction. Its units are magnitudes. For VS 17, the most precisely measured source with strong ice band extinction, our measures show that $\frac{\Delta m(3.013)}{\Delta m(3.108)} = 0.965 \pm 0.016$, just as expected for a band caused by water ice in thin mantles.

Our measure of the BN point source in Orion further tests the filter system's sensitivity to ice band extinction. For BN, $\Delta m(3.07) = 1.20 \pm 0.08$, which is

0.77 ± 0.10 of the $\Delta m(3.07)$ in the spectra of Gillett et al. (1975) and Merrill et al. (1976). Considering the estimated band profile, a compromise for the estimated response of our filters is $85 \pm 5\%$ of the true $\Delta m(3.07)$. The appropriate response correction is included in our tabulated ice measures.

Table XII presents the corrected ice band extinction measures. As mentioned previously, the photometry is based on comparisons of program stars with nearby unreddened stars. The continuum level at the position of the ice band is estimated from a series of polynomial fits to the other filter measures. The degrees of the polynomial fits are given in Table XII, as are the ratios $\Delta m(3.07)/E_{HK}$ and $\Delta m(3.07)/A_V$. Much of the uncertainty in the values of $\Delta m(3.07)$ and the ice ratios is due to uncertainty in the continuum level set by the polynomial fits. Uncertainties in estimating A_V make $\Delta m(3.07)/E_{HK}$ the preferred measure of relative ice extinction. Figure 15 shows a plot of the relative ice extinction against E_{HK} . The plot is quite remarkable. For $E_{HK} \lesssim 2.2$ ($A_V \lesssim 25$) the stars show no significant ice band extinction (except for HD 147889 which may be anomalous), while for $E_{HK} \gtrsim 2.2$ all of the stars yet measured show strong ice bands. The ice band data for those heavily obscured stars showing ice (although

TABLE XII^a

The Ice Band Extinction Measures

Name	O.P. ^b	$\Delta m(3.08)$	E_{HK}	$\frac{\Delta m(3.07)}{E_{HK}}$	$\frac{\Delta m(3.07)}{A_V}$
HD 147889	1,2,3	0.040 \pm .011	0.37	0.107 \pm .030	+0.0088 \pm .0025
SR 3	1,3	0.008 \pm .010	0.52	0.017 \pm .020	0.0013 \pm .0015
GS 31	1,2,3	0.032 \pm .015	0.78	0.042 \pm .020	0.0027 \pm .0015
GS 32	1,2,3	0.028 \pm .030	1.52	0.018 \pm .020	0.0016 \pm .0020
GS 26	1,3	0.175 \pm .060	2.21	0.079 \pm .030	0.0067 \pm .0025
VS 18	1,2,3	1.05 \pm .10	2.44	0.429 \pm .040	0.038 \pm .0035
GS 30	1,3	0.694 \pm .07	2.76	0.251 \pm .025	0.021 \pm .002
VS 17	1,2	1.05 \pm 0.10	3.13	0.336 \pm .035	0.029 \pm .003
VS 26	1,2	3.1 \pm 0.5	4.61	0.670 \pm .11	0.058 \pm .015
HD 168607	1,2	+0.033 \pm .030	0.49	0.068 \pm .061	0.0059 \pm .0053
VI Cyg 12	1,2	+0.025 \pm .015	0.61	0.041 \pm .025	0.0026 \pm .0016
NGC 2024 ^c					
#1		0.0 \pm 0.04	0.63	0.0 \pm 0.06	0.0 \pm 0.005
#2		1.3 \pm 0.1	2.87	0.45 \pm 0.05	0.041 \pm 0.005
BN ^d		1.57 \pm 0.04	4.4	0.36 (\pm 0.04)	0.03 (\pm 0.01)
Galactic ^e Center (2 μ m)		0.0 \pm 0.1	1.7	0.0 (\pm 0.06)	0.0 (\pm 0.01)

TABLE XII Continued

-
- a. All measures of obscuration are in magnitudes.
 - b. O.P. is the order of the polynomials used in estimating the continuum level at $3.07\mu\text{m}$.
 - c. For NGC 2024 #1 and #2, $\Delta m(3.07)$ is from Merrill et al. (1976) and E_{HK} and A_V are from Grasdalen (1974).
 - d. For BN the value of $\Delta m(3.07)$ is an average of the values in Table XI, E_{HK} is an estimate using photometry by Rieke for the present study and A_V is from Grasdalen (1974).
 - e. For the Galactic center $2\mu\text{m}$ source the $\Delta m(3.07)$ is estimated using data in Soifer, Russell and Merrill (1976) and E_{HK} is estimated using data from Becklin and Neugebauer (1968) and from Soifer et al. (1976).

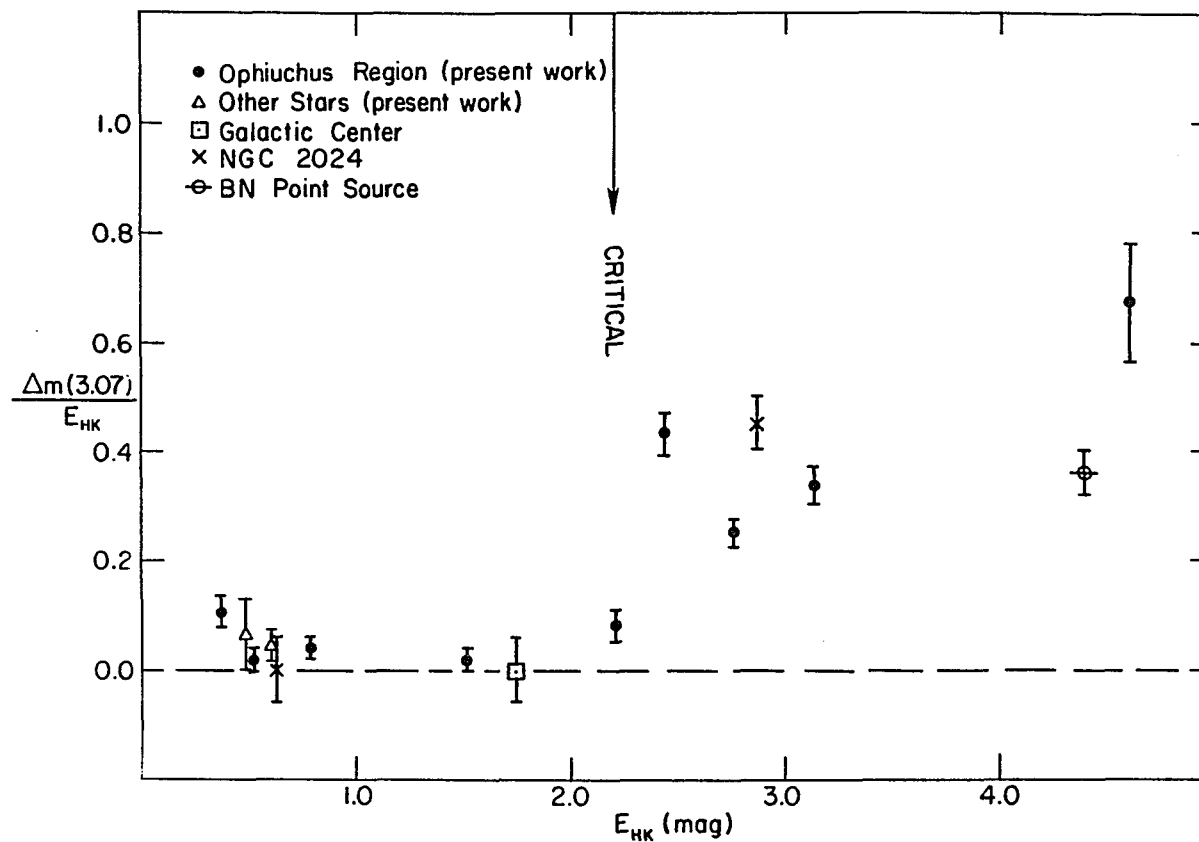


Figure 15. The dependence of the relative ice extinction on E_{HK} .

it is suggestive of an increase with E_{HK}) is inadequate to clearly establish a trend of relative band strength varying with E_{HK} . Above the onset of band extinction the relative band strength may well be constant.

Examining the extinction curves (Table X and Figure 13) along with the ice band data reveals that the onset of ice band extinction is not associated with any distinguishable anomaly in the shape of the continuum extinction. That is, in the more opaque regions of the Ophiuchus cloud the sources with, and the sources without measurable ice band extinction, have very similar, if not indistinguishable, IR extinction curves. This means that the continuum extinction gives no indication of the presence of ice or of changes in its abundance. Consequently, continuum extinction tells us nothing about the ice mantle thickness.

CHAPTER V

ANALYSIS OF THE INFRARED OBSERVATIONS

The Density Dependence of Ice Extinction

The apparent relation between the relative ice band strength $\Delta m(3.07)/E_{HK}$ and E_{HK} suggests the presence of a relation between the ice band strength and dust density. Cloud density should be an important variable in determining the amount of ice condensation because condensation is a recognized consequence of random encounters between gas atoms and grains (Oort and Hulst 1946, Wickramasinghe 1965, Greenberg 1968). At temperatures below the condensation temperature the standard model gives $\Delta m(3.07) \propto \int \rho^n ds$ with $n \approx 3$ (Greenberg 1968), where ρ is the gas plus dust space averaged density; while a measure of the continuum extinction such as E_{HK} behaves like $\int \rho ds$. Even if standard theory is incorrect and some other process controls the ice condensation, it is still likely that the gas and dust density will influence the ice formation process.

The value of E_{HK} can be directly related to density (monotonic) only if each source star is seen through just one dominant dust concentration (otherwise the number

of concentrations may be as important as the density). Therefore, since we see such a relation as we look through the Ophiuchus cloud, the particular condensation we look through is most likely the single source of major obscuration along our entire line of sight to the source star. (The cloud's proximity permits this.) The presence of just a few major obscuration centers is seen in the scale of the extinction correlation in the more opaque regions (data in Table X show a scale of ~ 0.4 pc) and in the scale of the projected radii of the three main regions where no stars are visible (see figures in Carrasco et al. 1973, and Vrba et al. 1975). Thus the apparent dust distribution and the presence of the relation between ice abundance and E_{HK} both support a model which has just a few major dust concentrations in the cloud and which is consistent with E_{HK} being directly related to dust density.

In the Ophiuchus cloud the critical value of E_{HK} for the presence of ice is ~ 2.2 mag and the scale of the dust concentrations is ~ 0.4 pc. Using these numbers, I computed an approximate critical density of 5 mag/pc in E_{HK} . Microwave studies show that in the dense portions of the cloud the gas density is $n \approx 10^5 \text{ cm}^{-3}$. (By way of contrast, the general interstellar medium in the galactic plane has an average density of $\sim 10^{-4.1}$ mag/pc in E_{HK}

and $n \approx 0.3 \text{ cm}^{-3}$.) The relatively large value of the critical density means that if this relation is generally applicable, then one should expect to find significant ice only in the densest regions. At lower densities, even when the extinction is large, there should be negligible ice. [The apparent absence of ice band extinction along the generally low density path toward the galactic nucleus, which has an $E_{\text{HK}} \approx 1.7$ (Becklin and Neugebauer 1968), is consistent with this concept (Soifer et al. 1976).]

To test whether the relation between apparent relative ice abundance and dust density is generally applicable one can examine measures of other source stars in regions where the extinction has been measured. Both HD 168607 and VI Cyg 12 are distant stars not associated with dense dust complexes. Although their extinction is strong by most standards (see Table VI), the extinction for both stars is well below that needed to give the critical density (even if all the extinction were concentrated in a 1 pc cloud), and as one would expect, our photometry shows no significant ice opacity (see Table XII). The density relation can also be tested for the two IR stars in NGC 2024 discussed by Grasdalen (1974). Here the estimated cloud scale is the 0.20 pc radius of the dust concentration visible on photos

of the nebula. This radius matches the radius of the neutral hydrogen cloud in the model of Grasdalen (1974). Using his values of E_{HK} for the two IR source stars, I found densities of ~ 3.2 and 15 mag/pc for NGC 2024 #1 and #2 respectively. As predicted by the relation found in Ophiuchus cloud, Grasdalen's measures show that #1 has no notable ice band extinction while #2 has strong ice band extinction. A similar, but weaker, argument can be made for the BN point source (cloud scale from Wilson, Jefferts and Penzias 1970), where the density is ~ 6.8 mag/pc in E_{HK} and ice is detected. Strom, Strom and Vrba (1976) and Strom, Vrba and Strom (1976) have reported ice band extinction measures for sources in dark clouds. Although these measures are of low statistical weight, they seem to be consistent with our derived relation for the Ophiuchus cloud. Our measures of extinction and $\Delta m(3.07)$ agree within the limits of our errors with those of Gillett et al. (1975) for VI Cyg 12 and the BN point source, confirming their supposition of a large variation of the ice band strength, and further affirming that the available data is consistent with the general applicability of the relative ice abundance-density relation found in Ophiuchus.

The Estimated Ice Fraction

The Absolute Ice Extinction Efficiency

The first requisite in order to use the measured values of $\Delta m(3.07)$ to estimate the ice mass fraction is a value for the absolute ice band extinction efficiency (cm^2/gm). The second requisite is a model of the wavelength dependent absolute extinction efficiency of the total assemblage of cloud particles.

Since our continuum extinction measures show no dependence on ice band strength, and the measured ice band profiles in other regions resemble absorption by bulk ice, it is reasonable to assume that in general when ice mantles are present they are thin enough to satisfy the Rayleigh approximation (at $3.07\mu\text{m}$). I have therefore used the Rayleigh approximation to compute the excess extinction of the ice band relative to the adjacent continuum extinction. Such a computation should closely describe the extinction by thin mantles on small to moderate size cores ($a \leq \lambda$), like those particles previously modeled (Chapter IV). Computing the net band extinction has required taking the difference in $\tau(3.07)$ between the band center and the average of the adjacent continuum, which required knowledge of the wavelength dependence of the complex refractive index ($m = n - ik$) across the band. Unfortunately the

complex refractive index, and the correlary absorption coefficient of ice, are not well determined near $3.07\mu\text{m}$, e.g., a comparison of the values given by Sill (1976) by Schaaf and Williams (1973) and by Bertie, Labbé, and Whalley (1969) with the compilation of data in Irvine and Pollack (1968) shows a factor of two range in the absorption index k . A compromise among these sources yields $m \approx 1.20 - 0.64i$ at the band opacity maximum. The opacity in the adjacent continuum is negligible compared to this. Of course this value ignores the possible effect of radiation damage which may significantly alter the complex refractive index both at the band center and in the adjacent continuum (Greenberg 1973). The expression for Rayleigh extinction is

$$\tau = \frac{18\pi V}{\lambda} \left[\frac{2nk}{(n^2 - k^2 + 2)^2 + (2nk)^2} \right],$$

where V is the volume of material per unit area of the beam integrated along the line of sight. Evaluating the bracket for both the band center and adjacent continuum and substituting for λ yields a measure of the absolute ice band sensitivity $[\Delta\tau(3.07)/V] \approx 2.4 \times 10^4 (\text{cm}^{-1})$. If $\rho_{\text{ice}} = 1\text{gm/cm}^3$ for grains in interstellar conditions, then $\Delta\xi(3.07) = \Delta\tau(3.07)/\rho V \approx 2.4 \times 10^4 \frac{\text{cm}^2}{\text{gm}}$. This satisfies the first requisite. Next comes the general

problem of modeling the extinction of the entire assemblage of cloud particles.

A Look at Grain Core Models

Unfortunately, deriving a model of the core grains in the Ophiuchus cloud is not as straightforward as one might assume. Specifically the difficulty is in using the available extinction observations, and some theoretical insight, to derive a general model of the grain composition and size distribution which can be used in computing the absolute extinction efficiencies. The difficulty can be seen upon examining the equation $\tau(\lambda) = \int \pi a^2 Q_e n_g da$, where n_g is the size dependent grain number density (cm^{-3}). If there are significant numbers of grains with widely differing values of $Q_e(\lambda)$, either because of composition or size differences, then the shape of the extinction curve $\tau(\lambda)$ becomes very sensitive to the size and/or composition of the particles. It should be emphasized that our ignorance of the particle size distribution cannot be separated from our ignorance of grain composition. Knowledge of one is needed to derive the other.

At least two distinct types or sizes of particles are recognizable in the extinction curves of the Ophiuchus stars: the optical extinction suggests the presence of small $[a \approx 0.13/(n-1)]$ particles only slightly larger than

normal interstellar grains, and the IR extinction points toward either small absorbing particles or large dielectric particles. The widely differing $Q_e(\lambda)$ dependences for large dielectric and small absorbing particles makes a grain composition model essential.

Assuming no major deviation from normal cosmic abundances (Allen 1964), I computed a series of grain models having the various compositions often put forth in the literature (e.g., silicates, graphite, etc.). The composition models were tested by comparing them with the Ophiuchus extinction observations scaled to the estimated H_2 density ($n \approx 10^5 \text{ cm}^{-3}$) and an assumed cloud dimension of ~ 0.4 pc. Within the errors of the model, all of the commonly proposed grain compositions are readily fitted to the Ophiuchus extinction observations by picking an appropriate grain size distribution (some models yield an excess of material and therefore a potential excess of extinction). However, exotic model particles (e.g., non-volatile hydrocarbons) do not seem to be abundant enough. Since the available observations cannot be used to give an unambiguous grain composition, theoretical argument is necessary.

A Look at Grain Growth Processes

The importance of distinctive particles to the IR extinction, and the apparent lack of similar distinctive particles in the general interstellar medium, force the assumption that, regardless of their composition, the IR extinction particles are formed in the cloud. There are two obvious means by which grains may grow in the cloud: either coatings may form on the grains, or the grains may stick on collision, yielding larger grains by coagulation (Lef  vee 1974; and Simons and Williams 1975). Unfortunately, observation cannot clearly distinguish between dominance by coating or coagulation. The extinction curves contain insufficient information to solve for the grain size distribution because information about grains in each element of space along the line of sight is lost in the average (Shifrin and Perelman 1967). Size dependent changes in $\xi(\lambda)$ are also lost in the average since they are masked by the much larger variations in the gross matter density.

However, a reasonable theoretical argument exists which shows that growth by coagulation is unimportant. Recent work (Greenberg 1977 and Hartmann 1976) on the fragmentation of various materials during particle-particle collisions has shown for likely interstellar grain materials a likely fragmentation velocity is

$v \approx 30$ meters/sec. For $v = 30$ m/sec, assuming the normal ratio of gas to dust, a gas density of 10^5 cm^{-3} and a particle size of $0.3 \mu\text{m}$, the time between particle-particle collisions is about $10^{5.3}$ years. At lower velocities, where fragmentation is unlikely, the time between collisions is so long that each particle experiences only a few collisions during the lifetime of the cloud. The other important variable in the collision-coagulation process is the sticking probability. Unfortunately, because of the uncertain physical properties of the grains, one cannot make an accurate model which leads to a meaningful sticking probability. However, a simple calculation shows that for a grain-grain collision at 10 m/sec there is no significant heating or melt welding at the collision surface. Thus it seems likely that the sticking probability is small and that coagulation is not effective as a grain growth process (Hartmann 1977). One interesting consequence of the grain collisions is the likely production of small collision fragments which could become the condensation nuclei for new grains. This effect may be quite significant if there are large grain velocities ($v > 100$ m/sec) in dense dark clouds.

A Model of the Grain Composition

Even without being certain that coating is the prevailing grain growth process it is possible to say something about the grain composition. The potentially abundant non-volatile substances are in two groups: carbon dominated or oxygen dominated. The molecular line observations and gas chemistry models say that carbon is mostly in the form of CO and some volatile complex molecules (Aannestad 1973; Watson and Salpeter 1972; Herbst and Klemperer 1976; and Oppenheimer and Dalgarno 1975). Therefore the cosmically abundant material which most likely constitutes the grains must be a mixture of highly non-volatile oxygen compounds such as silicates and metal oxides. One can also argue that much of the interstellar medium has been processed through dense clouds at least once during the life of the galaxy (Roberts 1969, Shu 1973, Shu 1975 and Appenzeller 1975). Therefore the distinctive IR extinction particles could be important contributors to the general interstellar extinction. If the IR extinction particles are composed of absorbing substances (e.g., graphite, Fe or SiC), then since such materials are generally metallic and non-volatile and the particles are relatively small (remember a $\lesssim 0.06\mu\text{m}$), they should readily survive to mix with the general interstellar medium. Therefore the seemingly well established dielectric nature of the normal interstellar particles

(Gehrels 1967; Vanýsek 1969; Hanner 1971; Martin, Illing and Angel 1972; and Zellner 1973) seems to argue persuasively against the significant presence of absorbing grains in dark clouds. On the other hand, if the IR extinction grains are large dielectrics, then although they should also be nonvolatile, grain destruction (which probably increases with grain size, e.g., $-\frac{dN}{dt} \propto a^2$, Greenberg 1966) may act on the grains to reduce their mean size. Thus if the IR extinction grains are large dielectrics, they may be the dominant source of grains which contribute to the pool of general interstellar medium particles.

If coagulation is a significant grain growth process then the IR grains should have the same composition as the small, presumably dielectric, grains from which they grow and the two distinct grain types in the cloud then differ only in size. However, it is much more likely that grain growth is by coating, since below a gas temperature of about 100°K all metal atoms stick to the grains, and in the presence of oxygen the result is substances composed of oxides like SiO_2 , Al_2O_3 , etc. (Watson and Salpeter 1972; and Aannestad 1973). I am aware of nothing which inhibits this process except perhaps the depletion of metals or oxygen or the presence of strongly ionizing radiation. Such a growth process is supported by the finding by Knapp,

Kuiper and Brown (1976) of a substantial reduction in the abundances of Si, Fe and Mg in the dense gas of the Ophiuchus cloud, presumably due to depletion onto the grains.

It seems that the least exotic grain model, and the one which best fits both observation and theory, has silicates in combination with metal oxides as the principal grain constituents, with perhaps small quantities of graphite and carbon compounds, and with some ice in the heavily obscured regions. The model assumes that Si, Mg, Al, Fe, Ca, etc. are in combination with oxygen in the oxidation states found in chondrites (Wood 1975), the dominant forms being minerals like pyroxene and olivine which are analyzed in terms of component oxides like SiO_2 , Al_2O_3 , and FeO . It is further assumed that there is no excess of the metallic elements beyond that in their chondritic compounds, none being in the gas or other molecules. The model also assumes that most of the carbon is in CO. The silicate-metal oxide model matches the above mentioned expectation of dominance by refractory dielectric particles. By direct comparison the model shows that (for $n_{\text{H}_2} = 10^5 \text{ cm}^{-3}$ over a path of ~ 0.4 pc) there is approximately the correct amount of material to fit the measured extinction. For an average silicate-metal oxide material a reasonable complex refractive index is $m \approx 1.55 + 0.01i$ and a reasonable density is

$\sim 3\text{gm/cm}^3$, for both the large and small grains. To estimate the maximum available ice abundance I computed the ratio $(\bar{\rho}_{\text{ice}}/\bar{\rho}_{\text{sil}})$, the space averaged density ratio of ice to silicates and metal oxides, on the assumption that all the oxygen left after CO, silicates, and metal oxides is in the form of ice. The resulting maximum $(\bar{\rho}_{\text{ice}}/\bar{\rho}_{\text{sil}})$ is ~ 0.7 .

The Problem of Large Grains

With a credible grain composition model in hand it seems to be time to set about modeling the grain size distribution. But there is the question, "Do very large grains contribute significantly to the aggregate grain mass?" This question must be considered first. In the limit $(a/\lambda) \rightarrow \infty$, $Q_e = 2$; and $\frac{dQ_e}{dm} = 0$, where m is the complex refractive index; all absorption bands are washed out; and the absolute extinction efficiency is $\xi = \frac{3}{2ap}\text{cm}^2/\text{gm}$. This is the geometric optics limit. It should be clear that a group of very large grains (e.g., $a \gtrsim 10\mu\text{m}$) may have substantial mass with no notable extinction or recognizable composition. Thus in the presence of such grains our extinction measures would not be representative of the aggregate grain mass.

Outside the dark clouds, in the general interstellar medium, measures of grey extinction in the optical and near

IR regions made by matching the extinction curve fit models with extinction measured by cluster diameters (see Chapter II), show that at most only a small fraction of the extinction is due to very large grains ($a \gtrsim 10\mu\text{m}$). Cosmic abundances also argue against a significant fraction of the mass being in very large grains. Thus, if there are such large grains in dark clouds, they surely form in the clouds. The abundance-based composition models give no indication that there might be a significant mass in excess of that seen by extinction observations, except in the case of H_2O ice, and for H_2O ice the band profiles and other observations clearly demonstrate its small abundance. Since there is no good reason to suspect the presence of very large grains, I have assumed that essentially all of the grain mass is in the grains seen by the extinction measures.

The Grain Size Distribution Model

Having put aside the question of very large grains it is now possible to approach the problem of the size distribution of visible grains. Since the Ophiuchus extinction curves cover only a moderate range in $1/\lambda$, only a simple model distribution is justifiable. I have approximated the size distribution using the two distinctive grain sizes: The small grains [with $a = 0.12/(n-1) \simeq 0.23\mu\text{m}$] and the

large IR grains [with $a = 0.26/(n-1) \approx 0.48\mu\text{m}$]. The size distribution then reduces to a single number, the ratio of the number densities of the two grain sizes averaged over the volume along the line of sight.

In order to estimate the number density ratio requires at least two observable extinction values whose ratio is sensitive to grain size. The ratio (A_V/E_{HK}) seems most suitable for this purpose because A_V is relatively insensitive to grain size for $a \gtrsim 0.15/(n-1)$ while E_{HK} is large for the IR grains and is small for the small grains. Table XIII gives the extinction efficiency values (Wickramasinghe 1973) used in the model to evaluate the expression

$$\frac{A_V}{E_{\text{HK}}} \approx \frac{\int \pi a^2 Q_e(0.55) n_g(a) da}{\int \pi a^2 (Q_e(1.6) - Q_e(2.2)) n_g(a) da}.$$

TABLE XIII

Grain Characteristics

	Small grains	IR grains
$Q_e(\lambda = 0.55 \text{ m})$	3.3	3.0
ΔQ_{HK}	0.13	1.16

I have assumed that for both large and small grains $m \approx 1.55 - .01i$. For the stars showing the distinctive IR

extinction $A_V/E_{HK} \cong 11.6$, so the ratio of the number density of small grains to IR grains (N_S/N_{IR}) is ~ 25 . The number ratio is linearly dependent on A_V/E_{HK} , showing that an error in estimating A_V should not grossly affect the computed number ratio. The ratio is also insensitive to small variations in m and a . Using this ratio and the tabulated extinction efficiencies I computed the (H-K) absolute extinction efficiency of the model grains,

$$\Delta\xi_{sil} = \xi(1.6) - \xi(2.2),$$

$$\Delta\xi_{sil} = \frac{3}{4\rho} \left[\frac{(\Delta Q_{HK})_S}{a_S} N_S + \frac{(\Delta Q_{HK})_{IR}}{a_{IR}} N_{IR} \right] / (N_S + N_{IR}).$$

The result is $\Delta\xi_{sil} = 0.16 \times 10^4 \text{ cm}^2/\text{gm}$, for silicate-metal oxide grains.

The Ice Mass Fraction

With estimates of both $\Delta\xi_{sil}$ and $\Delta\xi(3.07)$ in hand it is a straightforward proposition to solve the equation:

$$\left(\frac{\bar{\rho}_{ice}}{\bar{\rho}_{sil}} \right) = \frac{\Delta\xi_{sil}}{\Delta\xi(3.07)} \left[\frac{\Delta m(3.07)}{E_{HK}} \right],$$

with the result that $(\bar{\rho}_{ice}/\bar{\rho}_{sil}) \cong (0.066)[\Delta m(3.07)/E_{HK}]$. From Table XII come the various values of the extinction

ratio $[\Delta m(3.07)/E_{\text{HK}}]$. Substituting shows that for the less obscured sources showing no significant ice ($E_{\text{HK}} \lesssim 2.2$), that (except for HD 147889 which may be peculiar) $(\bar{\rho}_{\text{ice}}/\bar{\rho}_{\text{sil}}) = \sim 2 \times 10^{-3}$, and for the more heavily obscured sources $(\bar{\rho}_{\text{ice}}/\bar{\rho}_{\text{sil}})$ ranges from 1.7×10^{-2} to 4.4×10^{-2} . As mentioned previously the silicate-metal oxide model yields a maximum expected value of $(\bar{\rho}_{\text{ice}}/\bar{\rho}_{\text{sil}}) \approx 0.7$. Thus in the less obscured regions of the Ophiuchus cloud the relative ice abundance is ~ 350 times less than the maximum expected value and even in the dense regions showing ice, the relative ice abundance is ~ 30 times less than the maximum expected.

For comparison, it is interesting to note that for the BN point source the silicate ($10\mu\text{m}$) feature and ice feature have similar strengths. Using the above value of $2.4 \times 10^4 \text{ cm}^2/\text{gm}$ for ice and $\sim 3 \times 10^3 \text{ cm}^2/\text{gm}$ for silicate (Day 1976) yields a silicate to ice mass ratio of ~ 8 .

It should be emphasized that since we view the source stars through regions of greater and lesser opacity our view is undoubtedly through regions of greater and lesser ice density, so the natural tendency is to underestimate the relative ice abundance. Unfortunately, the amount of the underestimation cannot be determined because

of our ignorance of the detailed mass distribution in dense regions.

The uncertainties in estimating the relative ice abundance include the fact that other species may contribute to the apparent ice band extinction, that the band strength may depend on the composition of the mixture containing ice, that the ice band complex refractive index is uncertain, that the apparent ice abundance must be compared with an uncertain model of the core grain composition and size distribution, and that the conditions and ice abundance vary along the line of sight tending to cause underestimation of the ice abundance. Considering all of these uncertainties the estimated uncertainty in the relative ice abundance is a factor of ~ 3 . Even with this uncertainty, ice seems to be grossly under abundant for densities less than about 5 mag/pc in E_{HK} and significantly under abundant even for higher densities.

In the light of this knowledge it is apparent that the large measured values of R and λ_{\max} of polarization for HD 147889 and SR 3, the implied large R values for GS 31 and GS 32, and the associated distinctive extinction curves of all the IR source stars, are not due to the coating of grains with water ice. These peculiarities probably result from growth of silicate-metal oxide grains either by coating or coagulation.

The Ice Mantle Thickness

A useful application of the bi-modal silicate grain model is its use to estimate an average thickness of the ice mantles coating the grains. Considering that once a grain is coated by a monolayer of ice, other colliding atoms should see it as indistinguishable from other coated grains, it would seem likely that those grains with mantles have mantle thicknesses which are relatively uniform from grain to grain (provided there are no selective destruction processes). Furthermore, the small ratio of ice mantle mass to core mass suggests a small mantle thickness and suggests the utility of the approximation that the mantle volume is the core grain area (area = $4\sigma_c$, where σ_c is the cross section) times the average mantle thickness (δ). In that case,

$$\frac{\Delta m(3.07)}{E_{HK}} \cong \frac{(2.4 \times 10^4) \rho_{ice} (4\sigma_c \delta) n_g}{\sigma_c \Delta Q_{HK} n_g}$$

Again using the extinction efficiencies in Table XIII, for stars showing measurable ice, $\delta \approx 0.01\mu\text{m}$, indeed a small average mantle thickness. Since the simple bi-modal grain model ignores the possibly significant surface area contribution of very small grains (e.g., graphite with a $\sim .02\mu\text{m}$ to explain the $4.6\mu\text{m}^{-1}$ feature in the vacuum

UV), the present estimate of δ is in reality an estimate of the upper limit of the average mantle thickness. This tells us that in general ice mantles behave like Rayleigh particles even at optical wavelengths.

The Mantle Contribution to Continuum Extinction

Using the ice refractive index $m = 1.32 - ki$, ($k \ll 1$), in the near IR, the Rayleigh approximation yields $[A_K(\text{ice})/\Delta m(3.07)] \cong 2.0k$ (where $A_K = E_{K\infty}$). If in the near IR region the absorption is not extreme, then $k \leq 0.01$, and $[A_K(\text{ice})/\Delta m(3.07)] \leq 0.02$. Comparing with the data in Table X and in Table XII it is apparent that $[A_K(\text{total})/\Delta m(3.07)] \cong 3.5$, and that at most $\sim 1/200$ of A_K is due to the presence of ice mantles, even in the most heavily obscured regions. This explains why there is no change in the extinction curves associated with the onset of ice band extinction.

Why is There No Ice?

The students of the molecular and ionic chemistry of dark clouds seem to be agreed about the utility of ionic gas phase reactions in model making (Fertel and Turner 1975; Turner and Heiles 1974; Watson and Salpeter 1972; and Herbst and Klemperer 1976) and about the large abundance of complex molecules in the clouds, which together suggest the

action of an agent that inhibits the condensation of atoms and molecules on grain surfaces (Watson and Salpeter 1972; Herbst and Klemperer 1976). The current finding of little ice except in the densest regions also points toward the action of a condensation inhibitor effective against volatile substances. This brings up the question, "Which mechanisms affect the formation of molecules and their coating on grains?"

One obvious possibility is the effect of ionizing radiation. I have modeled the galactic diffuse ionizing radiation using current spectra and cross sections for both cosmic rays and X-rays (Garcia-Munoz, Mason and Simpson 1975; Davidson et al. 1972; Williamson et al. 1974; and Cruddace et al. 1974). For gases in low density regions ($A_V \lesssim \frac{1}{2}$) I find that the cosmic rays and X-rays produce comparable ionizations totalling $\sim 10^{-16.8} \text{sec}^{-1}$ which fits well with determinations by other methods (Fowler, Reeves and Silk 1970; Hobbs 1974; Jura 1974; Glassgold and Langer 1974; O'Donnell and Watson 1974; and Hainbach, Schramm and Blake 1976). In dense regions ($A_V \gtrsim 5$) the models show that gas ionization is dominated by cosmic rays ($\zeta \sim 10^{-17.3} \text{sec}^{-1}$, the probability per second that an atom will be ionized) while X-rays produce the major portion of the ionizations in grains ($\zeta \sim 10^{-16.0} \text{sec}^{-1}$),

These computed ionization rates are too small to produce any anomaly in either the gas phase chemistry or the condensation equilibrium. For comparison it is assumed that if there are many ionizations of each grain atom during the life of the cloud ($\sim 10^7$ yrs.) then the chemistry and/or condensation equilibrium will be affected ($\xi \gtrsim 10^{-12} \text{sec}^{-1}$). I have also modeled the ionizing radiation from the stars in and near the ρ Oph cloud. Still assuming they are normal main sequence stars, their ultraviolet and optical radiation should be strongly attenuated near the stars ($\tau_V = 1$ in ~ 0.02 pc) and should not escape into the general volume of the cloud. The stellar cosmic ray fluxes should also be negligible. However, the highly uncertain flux of stellar X-rays may be comparable to the diffuse X-ray flux. Even so, the maximum resulting ionization in the grains ($\sim 10^{-15.7} \text{sec}^{-1}$) is much less than that needed to affect the condensation equilibrium ($\sim 10^{-12} \text{sec}^{-1}$).

It has been suggested that dirty grain surfaces and impurities may interfere with molecular adsorption and crystal growth (Watson and Salpeter 1972). The inference is that a clean layer of pure substance is needed before a crystal can grow. However, such a statistical process should not have the observed sharp onset density of condensation.

In the less dense portions of the Ophiuchus cloud H_2O may be converted to other substances via the action of UV radiation, but in the regions where $A_V \gtrsim 10$ such an effect should be negligible. Thus UV conversion cannot explain the low ice abundance seen for most of the Ophiuchus stars.

One mechanism which might explain the low ice abundance is the combination of oxygen in another form such as a more volatile species or water of hydration. In the first instance, the high chemical stability of H_2O argues against the necessarily reversible chemical conversion process needed to explain adjacent regions with and without measurable ice. As to water of hydration, it seems highly improbable that at the low temperatures of the cloud, the density or temperature could so critically affect the binding of H_2O in crystals.

Another possibility I considered is that IR radiation from the stars may penetrate into the general volume of the cloud with sufficient intensity to remove molecules from the grain surfaces. However, even for the expected flux of $\sim 10^8$ photons/cm²sec between $\lambda = 1$ and $10\mu\text{m}$, since most photons should be ineffective at liberating molecules, this flux is most likely inadequate to affect the condensation equilibrium.

The most credible explanation I have seen thus far is that the dust is too hot for condensation of H_2O . Both Watson and Salpeter (1972) and Aannestad (1973) give a condensation temperature of $\sim 17^\circ K$, and as noted previously the observed dust temperature is $\sim 50^\circ K$ (Fazio et al. 1976). Thus one should expect to see no ice. Perhaps the small quantity of ice seen in the densest regions is permitted because those dense regions are significantly colder than the average dust in the cloud. [On the other hand if the gas is nearly adiabatic (weakly radiation coupled), then the temperatures in dense regions would be higher than their surroundings.]

Realizing that the process which heats the dust to $\sim 50^\circ K$ is not well understood, posit that there is a large energy input to the grains from the starlight absorbed in dust near the stars, and that this energy is converted by those grains to IR radiation which is weakly absorbed by the grains in the bulk of the cloud, elevating their temperatures. If such were the case, then the denser and more opaque regions would be colder because of self-shielding of this IR radiation, permitting the observed ice condensation. Recently Aannestad (1975) noted that the emissivity of ice in the thermal (at $\sim 50^\circ K$) region is larger than that of the expected silicate core particles.

This suggests the possibility that once a layer of ice forms, the grain cools, causing enhanced condensation. Such a critical process, in combination with self shielding of IR radiation, might explain the observed dependence of ice abundance on density. Even having this apparent explanation we cannot be sure that there are not other processes which may be influencing the condensation equilibrium.

CHAPTER VI

SUMMARY

Knowledge of the interstellar grains is important to many astronomical researches, yet current knowledge of the grain properties may be described as rudimentary. Information theory demonstrates that it is best to approach questions about the grain properties in the simplest possible fashion. Two questions were selected for study, expecting that they could be approached directly and simply: The question of the reality of the large reported variations in R ($\equiv A_V/E_{BV}$) and inferred grain size, and the question of the abundance of H_2O ice in interstellar grains. These questions are related since it has often been suggested that variation of apparent grain size may be due to variation of ice coating thickness.

A careful analysis of the diameters of 156 open clusters with modern photometry and angular diameter measures by Trumpler shows that the local galactic mean value of R is $\bar{R} = 3.15 \pm 0.20$. Further analysis shows that cluster diameter varies with both cluster concentration and number of recognized members. The mean cluster diameter, inferred value of R and the related mean grain

size seem not to depend on galactic longitude or position in space. However, since the cluster diameter method depends on diameter statistics, the present finding of no variation is valid only on a scale exceeding the width of the local spiral arm.

Infrared photometry of eleven strongly obscured stars shows that near ρ Oph the continuum extinction is distinctive, showing a large value of R and implied grain size. Precise measures ($\sigma \approx 0.01$ mag) the H_2O ice band (at $3.07\mu m$) show that for stars with $A_V \lesssim 25$ mag there is little or no ice extinction, the ratio of ice extinction to E_{HK} being an average 0.02 ± 0.02 , and for more heavily obscured stars the ice extinction to E_{HK} ratio is ~ 0.30 . These observations suggest a relation between ice extinction strength and dust density where regions with less than ~ 5 mag/pc in E_{HK} show negligible ice and more dense regions show significant ice extinction. The relatively low ice abundance even in the densest regions shows that the implied large grain size in Ophiuchus, is not due to the coating of grains by H_2O ice, instead it may be the result of coating of the grains by silicate material.

Using cosmic abundances and an assumed silicate core grain model, the maximum expected ice abundance was computed assuming all oxygen in excess of that combined in

silicates and CO is in the form of H_2O ice. Taking the ice extinction efficiency to be $2.4 \times 10^4 \text{ cm}^2/\text{gm}$ yields for for the less dense regions a computed ice to silicate ratio ~ 350 times less than the expected maximum. The most heavily obscured stars show an ice to silicate ratio ~ 30 times less than expected.

Upon critically examining processes which might inhibit ice formation or condensation it has been found that the relatively high dust temperature ($\sim 50^\circ\text{K}$) most likely prevents condensation of ice since condensation is generally believed to occur around 17°K . The apparent onset of ice condensation in dense regions suggests the possibility that condensation occurs because grains in dense regions are for some reason colder than in the bulk of the cloud.

REFERENCES

- Aannestad, Per A. 1973, Ap. J. Supp. 25, 205.
- Aannestad, Per A. 1975, Ap. J. 200, 30.
- Aannestad, Per A. and Edward M. Purcell 1973, Ann. Rev. Aston. and Ap. 11, 309.
- Allen, C. W. 1964, Astrophysical Quantities, (London: William Clowes and Sons Ltd.).
- Appenzeller, I. 1975, Conf. on Optical Observing Programs on Galactic Structure and Dynamics, ed. Th. Schmidt-Kaler (Astronom. Inst. of Ruhr-Univ.).
- Bardwell, J. and C. Sivertz 1947, Can. J. Res. 25B, No. 3, 255.
- Becker, W. 1963, Zeitschrift für Ap. 57, 117.
- Becker, W. 1966, Zeitschrift für Ap. 64, 77.
- Becklin, E. E. and G. Neugebauer 1968, Ap. J. 151, 145
- Bertie, J. E., H. J. Labbé, and E. Whalley 1969, J. Chem. Phys. 50, 4501.
- Blaauw, A. 1963, Stars and Steller Systems, ed. K. A. Strand (Chicago: Univ. of Chicago Press) Vol. 3, Ch. 20.
- Bok, Bart. J. 1956, A. J. 61, 309.
- Breda, I. G. van, I. S. Glass, and D. C. B. Whittet 1974, M.N.R.A.S. 168, 551.
- Brown, R. L., R. H. Gammon, G. R. Knapp, and B. Balik 1974, Ap. J. 192, 607.
- Brown, R. L. and B. Zukerman 1975, Ap. J. (lett.) 202, L125.
- Cameron, A. G. W. 1975, The Dusty Universe, ed. George B. Field and A. G. W. Cameron (New York: Neale Watson Academic Pub.), p. 1.

- Carrasco, L., S. E. Strom, and K. M. Strom 1973, Ap. J. 182, 95.
- Chaisson, E. J. 1975, Ap. J. (lett.) 197, L65.
- Chaldu, R., R. K. Honeycutt, and M. V. Penston 1973, P.A.S.P. 85, 87.
- Cohen, Martin 1976, Ap. J. 203, 169.
- Coyne, G. V., S. J., T. Gehrels, and K. Serkowski 1974, A. J. 79, 581.
- Crawford, D. L., and J. V. Barnes 1970, A. J. 75, 952.
- Crudace, Raymond, Francesco Paresce, Stuart Bowyer, and Michael Lampton 1974, Ap. J. 187, 497.
- Davidson, A., S. Shulman, G. Fritz, J. F. Meekins, R. C. Henry, and H. Friedman 1972, Ap. J. 177, 629.
- Day, Kenrick L. 1976, Ap. J. (in press).
- Day, Kenrick L., and Donald R. Huffman 1973, Nature Phys. Sci. 243, 50.
- Danielson, R. E., N. J. Woolf, and J. E. Gaustad 1965, Ap. J. 141, 116.
- de Vries, M. 1972 (unpublished, Kapteyn Sterrewacht, Roden, Holland).
- Encrenaz, P. J. 1974, Ap. J. (lett.) 189, L135.
- Fazio, G. G., E. L. Wright, M. Zeilick II, F. J. Low 1976, Ap. J. (lett.) 206, L165.
- Fertel, J. H., and B. E. Turner 1975, Astrophysical Letters 16, 61.
- Fowler, W. A., H. Reeves, and J. Silk 1970, Ap. J. 162, 49.
- Frogel, J. A., S. E. Persson, M. Aaronson, E. E. Becklin, K. Matthews and G. Neugebauer 1975, Ap. J. (lett.) 195, L15.
- Garcia-Munoz, M., G. M. Mason, and J. A. Simpson 1975, Ap. J. 202, 265.

- Garrison, R. F. 1967, Ap. J. 147, 1003.
- Garrison, R. F. 1970, A. J. 75, 1001.
- Gaustad, J. E., F. C. Gillett, R. F. Knacke, and W. A. Stein 1969, Ap. J. 158, 613.
- Gehrels, Thomas 1967, A. J. 72, 631.
- Gillett, F. C., and W. J. Forrest 1973, Ap. J. 179, 483.
- Gillett, F. C., T. W. Jones, K. M. Merrill, and W. A. Stein 1975, Astron. and Ap. 45, 77.
- Glaspey, John W. 1971, Ph. D. Dissertation Univ. of Arizona.
- Glassgold, A. E., and W. D. Langer 1974, Ap. J. 193, 73.
- Gordon, M. A., and L. E. Snyder 1973, Molecules in the Galactic Environment (New York: John Wiley and Sons).
- Grasdalen, G. L. 1974, Ap. J. 193, 373.
- Grasdalen, G. L., R. Joyce, R. F. Knacke, S. E. Strom, and K. M. Strom 1975, A. J. 80, 117.
- Grasdalen, G. L., K. M. Strom, and S. E. Strom 1973, Ap. J. (lett.) 184, L53.
- Greenberg, J. Mayo 1966, Ap. J. 145, 57.
- Greenberg, J. Mayo 1968, Stars and Stellar Systems, ed. Barbara K. Middlehurst and Lawrence H. Aller (Chicago: Univ. of Chicago Pres) Vol. 7, Ch. 6.
- Greenberg, J. Mayo 1973, IAU Symp. 52, Interstellar Dust and Related Topics, ed. J. Mayo Greenberg and H. C. van de Hulst (Dordrecht: Reidel), p. 3.
- Greenberg, Richard 1977, Icarus (in press).
- Grubissich, C. 1968, Zeitschrift für Ap. 68, 309.
- Grumprecht, R. O., and C. M. Sliepcevich 1953, J. Chem. Phys. 57, 90.
- Hagen, Gretchen L. 1970, Publ. David Dunlap Obs. 4.

- Hainbach, K. L., D. N. Schramm, and J. B. Blake 1976, Ap. J. 205, 920.
- Hall, Donald N. B., Richard S. Aikens, Richard Joyce, and Thomas W. McCurnin 1975, Applied Optics 14, 450.
- Hanner, Martha S. 1971, Ap. J. 164, 425.
- Hardie, R. H., and D. L. Crawford 1961, Ap. J. 133, 843.
- Hartmann, William K. 1976, (Planetary Science Inst., Tucson, Arizona) private communication.
- Hartmann, William K. 1977, Bull. Amer. Astron. Soc. (in Press).
- Heiles, C. 1973, Ap. J. 183, 441.
- Heller, W., J. N. Epel, and R. M. Tabibian 1954, J. Chem. Phys. 22, 1777.
- Herbst, Eric, and William Klemperer 1976, Physics Today 29, 32.
- Hiltner, W. A. 1956, Ap. J. Supp. 2, 389.
- Hobbs, L. M. 1974, Ap. J. (lett.) 188, L107.
- Huffman, Donald R. 1975, Ap. and Space Sci. 34, 175.
- Huffman, Donald R., and J. L. Stapp 1973, IAU Symp. 52, Interstellar Dust and Related Topics, ed. J. Mayo Greenberg and H. C. van de Hulst (Dordrecht: Riedel) p. 297.
- Hulst, H. C. van de 1957, Light Scattering by Small Particles (New York: John Wiley & Sons), p. 193.
- Hunter, C. E., and B. Donn 1971, Ap. J. 167, 71.
- Irvine, W. M., and J. B. Pollack 1968, Icarus 8, 324.
- Isobe, Syuzo 1968, Pub. Astr. Soc. Japan 20, No. 1, 52.
- Johnson, H. L. 1964, Bol. de Los Observ. Tonantzintla y Tacubaya 3, No. 25, p. 305.
- Johnson, H. L. 1967, Ap. J. 149, 345.

- Johnson, H. L. 1968, Stars and Stellar Systems, ed Barbara M. Middlehurst and Lawrence H. Aller (Chicago: Univ. Chicago Press) Vol. 7, Ch. 5.
- Johnson, H. L., A. A. Hoag, B. Iriarte, R. I. Mitchell, and K. L. Hallam 1961, Lowell Obs. Bull. 5, No. 8, p. 133.
- Johnson, H. L., R. I. Mitchell, B. Iriarte, and W. Z. Wisniewski 1966, Comm. Lunar and Planet. Lab. 4, No. 63.
- Jones, D. H. P. 1970, M.N.R.A.S. 152, 231.
- Jura, M. 1974, Ap. J. 191, 375.
- King, Ivan 1952, A. J. 57, 253.
- Knacke, R. F., D. D. Cudaback, and J. E. Gaustad 1969, Ap. J. 158, 151.
- Knapp, G. R., T. B. H. Kuiper, and Robert L. Brown 1976, Ap. J. 206, 109.
- LaMer, V. K. 1948, J. Phys. and Colloid. Chem. 52, 65.
- Lee, Thomas A. 1968, Ap. J. 152, 913.
- Lee, Thomas A. 1970, Ap. J. 162, 217.
- Lefévee, J. 1974, Astron. and Ap. 37, 17.
- Low, F. J., and G. Rieke 1976, Methods of Exper. Physics 12, 415.
- Lynds, Beverly T. 1967, P.A.S.P. 79, 448.
- MacConnell, D. J. 1968, Ap. J. Supp. 16, 275.
- Martin, P. G., R. Illing, and J. R. P. Angel 1972, M.N.R.A.S. 159, 191.
- Mathewson, Donald S. 1968, Ap. J. (lett.) 153, L47.
- McCuskey, S. W. 1965, Stars and Stellar Systems, ed. Adriaan Blaauw and Maarten Schmidt (Chicago: Univ. of Chicago Press), Vol. 5, Ch. 1.

- McNalley, D. 1973, IAU Symposium 52, Interstellar Dust and Related Topics, ed. J. Mayo Greenberg and H. C. van de Hulst (Dordrecht: Reidel), p. 549.
- Merrill, K. M., R. W. Russell, and B. T. Soifer 1976, Ap. J. 207, 763.
- Merrill, K. M., and B. T. Soifer 1974, Ap. J. (lett.) 189, L27.
- Merrill, K. M., and W. A. Stein 1976, P.A.S.P. 88, 285.
- O'Donnell, E. J., and W. D. Watson 1974, Ap. J. 191, 89.
- Oort, J. H., and H. C. van de Hulst 1946, B.A.N. 10, No. 376, p. 187.
- Oppenheimer, M., and A. Dalgarno 1975, Ap. J. 200, 419.
- Penzias, A. A. 1972, Ap. J. (lett.) 174, L43.
- Reeves, H. 1972, Symposium on the Origin of the Solar System (Paris: Centre National de la Recherche Scientifique).
- Rieke, George H. 1974, Ap. J. (lett.) 193, L81.
- Roberts, W. W. Jr. 1969, Ap. J. 158, 123.
- Rydgren, A. E., S. E. Strom, and K. M. Strom 1976, Ap. J. Supp. 30, 307.
- Schaaf, J. W., and D. Williams 1973, J. Opt. Soc. Am. 63, 726.
- Schultz, G. V., and W. Weimer 1975, Astron. and Ap. 43, 133.
- Serkowski, K. 1968, Ap. J. 154, 115.
- Serkowski, K. 1973, IAU Symp. 52, Interstellar Dust and Related Topics, ed. J. Mayo Greenberg and H. C. van de Hulst (Dordrecht: Riedel), p. 145.
- Serkowski, K., T. Gehrels and W. Wisniewski 1969, A. J. 74, 85.
- Serkowski, K., D. S. Mathewson, and V. L. Ford 1975, Ap. J. 196, 261.

- Shifrin, K. S., and A. Y. Perelman 1967, Electromagnetic Scattering, ed. Robert L. Rowell and Richard S. Stein, (London: Gordon and Breach), p. 131.
- Shu, Frank H. 1973, IAU Symp. 52, Interstellar Dust and Related Topics, ed. J. Mayo Greenberg and H. C. van de Hulst (Dordrecht: Reidel), p. 257.
- Shu, Frank H. 1975, La Dynamique des Galaxies Spirales Colloque Intern., Centre Nat. Res. Sci., No. 241.
- Silk, Joseph, and M. W. Werner 1969, Ap. J. 158, 185.
- Sill, Godfrey 1976, (Res. Assoc., U. of Ariz., Tucson) private communication.
- Simons, S., and I. P. Williams 1975, Ap. and Space Sci. 32, 493.
- Simonson, S., III 1968, Ap. J. 154, 923.
- Sinclair, David 1947, J. Opt. Soc. Amer. 37, 475.
- Snow, Theodore P. and Judith G. Cohen 1974, Ap. J. 194, 313.
- Soifer, B. T., R. W. Russell, and K. M. Merrill 1976, Ap. J. (lett.) 207, L83.
- Spitzer, Lyman 1968, Diffuse Matter in Space (New York: John Wiley and Sons, Inc.).
- Strom, K. M., S. E. Strom, Luis Carrasco, and Frederick J. Vrba 1975, Ap. J. 196, 489.
- Strom, K. M., S. E. Strom, and F. J. Vrba 1976, A. J. 81, 308.
- Strom, S. E., K. M. Strom, and L. Carrasco 1974, P.A.S.P. 86, 798.
- Strom, S. E., F. J. Vrba, and K. M. Strom 1976, A. J. 81, 314.
- Struve, Otto, and Mogens Rudkjøbing 1949, Ap. J. 109, 92.
- Trumpler, Robert J. 1922, Publ. Allegheny Obs. 6, No. 4, 45.
- Trumpler, Robert J. 1930, Lick Obs. Bull. 14, No. 420, p. 154.

- Turner, B. E., and C. E. Heiles 1974, Ap. J. 194, 525.
- Vanýsek, V. 1969, Vistas in Astronomy 11, 189.
- Voelcker, K. 1975, Astron. and Ap. Supp. 22, No. 1, p. 1.
- Vrba, Frederick J., Karen M. Strom, Stephen E. Strom, and G. L. Grasdalen 1975, Ap. J. 197, 77.
- Walborn, Nolan R. 1972, A. J. 77, 312.
- Walker, G. A. H. 1962, The Observatory 82, 52.
- Wallenquist, Åke 1959, Ann. Uppsala Obs. 4, No. 6.
- Watson, W. D., and E. E. Salpeter 1972, Ap. J. 175, 659.
- Whittet, D. C. B. 1974, M.N.R.A.S. 168, 371.
- Wickramasinghe, N. C. 1965, M.N.R.A.S. 131, 177.
- Wickramasinghe, N. C. 1967, Interstellar Grains (London: Chapman and Hall) p. 66.
- Wickramasinghe, N. C. 1973, Light Scattering Functions for Small Particles with Applications in Astronomy (New York: John Wiley and Sons, Inc.).
- Wickramasinghe, N. C., and K. Nandy 1972, Reports on Progress in Phys. 35, 157.
- Williamson, F. O., W. T. Sanders, W. L. Kraushaar, D. McCammon, R. Borken, and A. N. Bunner 1974, Ap. J. (lett.) 193, L133.
- Wilson, R. W., K. B. Jefferts, and A. A. Penzias 1970, Ap. J. (lett.) 161, L43.
- Wood, John A. 1975, The Dusty Universe, ed. George B. Field and A. G. W. Cameron (New York: Neale Watson Academic Pub.), p. 245.
- Zellner, Benjamin 1973, IAU Symposium 52, Interstellar Dust and Related Topics, ed. J. Mayo Greenberg and H. C. van de Hulst, (Dordrecht: Reidel), p. 109.